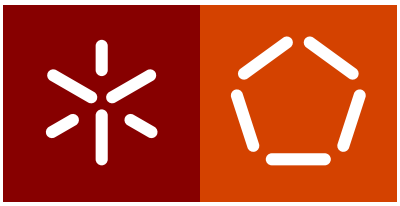

Universidade do Minho
Escola de Engenharia
Departamento de Informática

David Miguel Ferreira dos Santos

Dynamic genome-scale modelling of the *Saccharomyces* non-*cerevisiae* yeasts metabolism in wine fermentation

January 2021

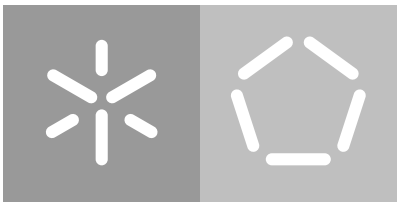

Universidade do Minho
Escola de Engenharia
Departamento de Informática

David Miguel Ferreira dos Santos

Dynamic genome-scale modelling of the *Saccharomyces* non-*cerevisiae* yeasts metabolism in wine fermentation

Master dissertation
Master Degree in Bioinformatics

Dissertation supervised by
Dr. Miguel Francisco Almeida Pereira Rocha
Dr. Eva Balsa-Canto

January 2021

DIREITOS DE AUTOR E CONDIÇÕES DE UTILIZAÇÃO DO TRABALHO POR TERCEIROS

ACKNOWLEDGMENTS

Numa breve reflexão, compreendo que este trabalho não seria concretizável sem a ajuda e o apoio de diversas pessoas, às quais dirijo os meus sinceros agradecimentos.

Primeiramente, à minha orientadora, Doutora Eva Balsa-Canto, agradecido por todo o tempo dispensado na partilha de conhecimentos e na integração no instituto, pelo apoio demonstrado desde o primeiro e-mail, pela disponibilidade, preocupação e simpatia que me ajudaram a crescer enquanto investigador e pessoa. *Muchas gracias*!

Ao meu orientador, Prof. Doutor Miguel Rocha, obrigado pela partilha de conhecimentos, sugestões e oportunidades que permite aos alunos experiências mais diversificadas.

Ao Doutor David Henriques, investigador do grupo, para além da preciosa ajuda a entender todo o processo de investigação deste trabalho, constante disponibilidade para esclarecer dúvidas e discutir ideias, ajudou-me na parte burocrática. Muito obrigado!

A todos os elementos do IIM-CSIC, obrigado por me acolherem como um de vós.

À família, que pergunta sempre quando é que começo a trabalhar, obrigado por serem o alicerce que me suporta nas minhas batalhas. Ao Pai e à Mãe, uma gratidão imensurável, por tudo que conseguiram/abdicaram para que eu pudesse chegar até aqui. Ao Edu, sabes que estou aqui para ajudar, grande beijinho.

À Angie, o meu refúgio, a pessoa que mais me compreende, incentiva, acredita em mim e nas minhas capacidades. Aliado à sua paciência, apreço e amor, muito obrigado!

Aos amigos, obrigado por marcarem presença nos momentos importantes, sejam eles alegres ou não. Em especial, ao Machado e ao Gil, pela extensa partilha de aventuras.

This work was supported by the CSIC (Consejo Superior de Investigaciones Científicas) through the “JAE Intro ICUs 2019” grant: JAEICU-19-IIM-01 (introduction grants to research for university students).

STATEMENT OF INTEGRITY

I hereby declare having conducted this academic work with integrity. I confirm that I have not used plagiarism or any form of undue use of information or falsification of results along the process leading to its elaboration.

I further declare that I have fully acknowledged the Code of Ethical Conduct of the University of Minho.

ABSTRACT

The wine industry is facing challenging times due, mostly, to climate change and changing consumer demands. The urge to innovate stimulates R&D of new fermentation processes using non-conventional yeast species (*e.g.* non-*cerevisiae Saccharomyces* species). While recent research approached the physiology of diverse non-conventional yeast species, little is known about their metabolism in different environmental conditions.

In this work, a previously developed dynamic genome-scale model was adapted to study the metabolism of *Saccharomyces kudriavzevii* in wine fermentation at two temperatures, 25°C and 12°C. Adjustments included the addition of metabolic pathways and dynamic constraints. Goodness-of-fit of the model to measurements of the extracellular compounds was satisfactory, *i.e.* the median values of R^2 are 0.95 and 0.87 for 25°C and 12°C, respectively.

The model was then used to explore the differences in the dynamics of metabolism between temperatures. The most significant differences appeared in the stationary phase: 1) the strain produces more mevalonate and succinate at 25°C, probably due to a late response to stress and the maintenance of redox balance via the GABA shunt, respectively, 2) erythritol flux is higher at 12°C, probably due to the conditions of formation lasting longer and 3) the production of higher alcohols, mostly *de novo*, is higher at 12°C, due to the longer viability of the cells.

The proposed model provided a comprehensive picture of the main steps occurring inside the cell during wine fermentation. Model predictions are consistent with experimental data and previous findings, but it also brought novel results, such as the role of the GABA shunt or the production of mevalonate in the metabolism of *S. kudriavzevii*, worth being explored further.

Keywords: fermentation, metabolism, modelling, *S. kudriavzevii*

RESUMO

A indústria vinícola atravessa tempos desafiantes, sobretudo devido às alterações climáticas e às mudanças das exigências dos consumidores. A necessidade de inovar estimula a I&D de novos processos fermentativos usando espécies de leveduras não convencionais, (*e.g.* espécies *Saccharomyces* não-*cerevisiae*). Apesar de investigações recentes abordarem a fisiologia de diversas espécies de leveduras não convencionais, sabe-se pouco sobre o seu metabolismo em diferentes condições ambientais.

Neste trabalho, adaptou-se um modelo dinâmico à escala genômica para estudar o metabolismo da *Saccharomyces kudriavzevii* CR85 durante a fermentação de vinho a 25°C e 12°C. Os ajustes incluem a adição de vias metabólicas e restrições dinâmicas. A adequação do modelo às medições dos compostos extracelulares foi satisfatória, *i.e.*, os valores medianos de R^2 são de 0.95 e 0.87 para 25°C e 12°C, respectivamente.

O modelo foi então utilizado para explorar as diferenças nas dinâmicas do metabolismo entre temperaturas. A maioria das diferenças significativas surgem na fase estacionária: 1) a estirpe produz mais mevalonato e succinato a 25°C, provavelmente devido a uma resposta tardia ao stress e à manutenção do balanço redox através da via alternativa do GABA, respectivamente, 2) fluxo de eritritol é maior a 12°C, provavelmente devido às condições da sua formação durarem mais e 3) a produção de álcoois superiores, sobretudo via *de novo*, é superior a 12°C, devido à longa viabilidade das células.

O modelo proposto permitiu um retrato completo dos principais passos ocorridos no interior da célula durante a fermentação de vinho. As previsões do modelo estão de acordo com os dados experimentais e descobertas anteriores, no entanto, também trouxe resultados inovadores, como o papel da via GABA ou a produção de mevalonato no metabolismo da *S. kudriavzevii*, que vale a pena ser mais explorado.

Palavras-Chave: fermentação, metabolismo, modelação, *S. kudriavzevii*

CONTENTS

ACRONYMS

ATP	adenosine triphosphate
BCAAs	Branched-Chain Amino Acids
bn	billion
BRENDA	BRaunschweig ENzyme DAtabase
CCM	Central Carbon Metabolism
CFU/L	Colony-Forming Unit per Litre
COBRA	COnstraint-Based Reconstruction and Analysis Toolbox
CSIC	Consejo Superior de Investigaciones Científicas
dFBA	dynamic Flux Balance Analysis
DNA	deoxyribonucleic acid
DOA	Dynamic Optimisation-based Approach
DW	Dry Weight
EU	European Union
EUR	Euro
FBA	Flux Balance Analysis
GABA	gamma-aminobutyrate
GAD1	glutamate decarboxylase gene
GEMs	genome-scale metabolic models
GMOs	Genetically Modified Organisms

GOLD	Genomes OnLine Database
GPR	Gene-Protein-Reaction
HTML	HyperText Markup Language
IATA	Instituto de Agroquímica y Tecnología de Los Alimentos
IVP	Initial Value Problem
KEGG	Kyoto Encyclopedia of Genes and Genomes
LP	Linear Programming
MATLAB	MATrix LABoratory
NCBI	National Center for Biotechnology Information
NGS	Next Generation Sequencing
NLPs	nonlinear programming problems
ODEs	Ordinary Differential Equations
pFBA	parsimonious Flux Balance Analysis
PPP	Pentose Phosphate Pathway
SB	Systems Biology
SBML	Systems Biology Markup Language
SGD	*Saccharomyces* Genome Database
SNR	Signal-Noise Ratio
SOA	Static Optimisation-based Approach
SuB	*Saccharomyces uvarum* BMV58
SuC	*Saccharomyces uvarum* CECT12600
T73	*Saccharomyces cerevisiae* T73
TCA cycle	tricarboxylic acid cycle

UniProt	Universal Protein Resource
UniProtKB	UniProt Knowledgebase
YAN	Yeast Assimilable Nitrogen

LIST OF FIGURES

LIST OF TABLES

1

INTRODUCTION

1.1 CONTEXT AND MOTIVATION

History gives a good perspective of the wine cultural importance, since its ”discovery” about 6000 years ago, has been commonly used in the human diet and on social and religious occasions. Moreover, wine is produced practically on all continents [1]. Ever since, as a common process, the marketing of wine started to happen.

The global wine market has witnessed steady growth over the years. In 2018, the sum of exports from all countries reached 31.3 bn EUR [2]. The European Union (EU) is the world-leading producer of wine. Between the campaigns 2009-2010 and 2018-2019, the average annual production was 159 million hectolitres. In 2018, it accounted for 43.5% of wine-growing areas, 62.9% of production, more than 60% of global consumption and 70.4% of exports, in global terms. Within the EU, France, Italy and Spain represent about 80% of the total production. Together, these three countries constitute 50.7% of wine producers of the world market, in volume terms. Other relevant EU producers include Germany, Portugal, Romania, Greece and Hungary [2–4].

Despite these figures, the EU wine industry is facing several challenges. Apart from the fierce international competition, with new producers appearing in different countries, internal EU consumption decreases, and climate change is affecting wine production globally [5, 6].

Consumers demand products with lower alcohol and fruiter aromas. At the same time, climate change has different effects on vine grapes, including lower acidity, phenolic maturation and altered tannin content, and notably higher sugar levels, which boost the alcohol content. Early harvest would avoid high sugar content in grape must and thus reduce the final alcohol content. However, it would prevent the optimal phenolic maturity and aromatic complexity required to produce the well-structured and full body wines consumers are demanding. The use of alternative yeast starters emerges as a possibility to face the challenge [7].

Winemaking is a conversion of grape juice made mainly by yeasts, led by *Saccharomyces cerevisiae*, were a vast number of compounds are metabolically consumed and produced. Modern wine-production relies on selected yeasts to inoculate grape must. The use of so-called starters allows to control the fermentation, reduce the risk of contamination, increase the reproducibility and generate specific wine characteristics. Most of the commercial starters are *S. cerevisiae*, therefore being the most frequently used in wine fermentation, as well as the most studied species. However, other species of the *Saccharomyces* genus have shown their potential application to solve the new challenges of the winemaking industry. Particularly, *Saccharomyces* non-*cerevisiae* yeasts, *S. uvarum* and *S. kudriavzevii*, or hybrids, *S. cerevisiae* x *S. uvarum* and *S. cerevisiae* x *S. kudriavzevii*, exhibit good fermentative capabilities at low temperatures, producing wines with lower alcohol and higher glycerol amounts and new aromatic profiles [7].

Still, the design of new wine fermentation processes requires a better understanding of the differences in fermentation behaviour between *Saccharomyces* non-*cerevisiae* yeasts and, how these characteristics can be modulated to enable increased scope and specificity in tailoring wine composition.

A systems biology-based approach has the potential to elucidate the origin of such differences through the integrative use of genome-scale metabolic networks, mathematical models and molecular omics data [8, 9].

Dynamic genome-scale metabolic models (GEMs) allow for the study of the metabolic response and flux simulation in a system of interest (*e.g.* bacteria, yeasts, algae, *etc*) under given environmental conditions. In a GEM, metabolites link to each other through reactions associated with enzymes encoded by genes. The stoichiometric matrix represents reactions, and it is used to define balance equations describing the dynamics of metabolic concentrations as a function of reaction rates (or fluxes). Metabolic fluxes can be then obtained by, for example, flux balance analysis (FBA) [10], which accounts for a specific cellular objective (*e.g.* maximum growth rate) plus specific constraints on internal and external fluxes. FBA can be solved iteratively to handle dynamic systems [11].

Agosin and co-workers proposed using dynamic GEMs to predict wine fermentation by a *S. cerevisiae* industrial species [12, 13]. Their models, based on the iFF708 reconstruction, which included 1175 metabolic reactions comprising 584 components [14], were able to reasonably explain the measured dynamics of biomass growth, hexoses uptake and ethanol and glycerol production [12, 13]. However, their models did not consider nitrogen metabolism in stationary and decay phases, in which the most extracellular accumulation of fusel alcohols happens, such as 2-phenylethanol, isoamyl alcohol and isobutanol, responsible for odour and flavour. Therefore, the models could not predict the production of aromas and other wine relevant metabolites.

Henriques et al. [15, 16] proposed an integrative genome-scale dynamic model of wine fermentation, which accounts for the dynamics of the consumption of carbon and nitrogen (organic and inorganic) sources, as well as aroma formation. For the modelling, the authors integrated a wine specific metabolic reconstruction, based on an extension of the current consensus genome-scale model of *S. cerevisiae* (Yeast8 [17]), into a dynamic kinetic model to account for the time-varying culture environment. Extracellular substrate concentrations were used to compute time-varying substrate uptake rates through kinetic expressions. The dynamics of extracellular products were modelled using kinetic models and used to constrain the problem further. The dynamics of intracellular fluxes were

computed using a dynamic implementation of a parsimonious flux balance analysis (pFBA [18]). The model was calibrated using experimental data from batch fermentations and used to explain the differences in the metabolism of *S. cerevisiae* and *S. uvarum* strains under wine fermentation conditions.

1.2 OBJECTIVES

This work aims to update that previously developed model to explain the metabolism of yet another *Saccharomyces* species: *S. kudriavzevii* CR85, and explore its metabolism under different fermentation temperatures.

More specifically, the work will address the following objectives:

- Explore the formulation of dynamic constraints: ordinary differential equations (ODEs) describing the dynamics of experimentally measured external metabolites;
- Explore the formulation and solution of the dynamic genome-scale models as implemented in AMIGO2 toolbox [19] and its interface with COnstraint-Based Reconstruction and Analysis (COBRA) toolbox [20];
- Obtain a dynamic genome-scale description of the metabolism of *S. kudriavzevii* CR85 for alternative temperature conditions during wine fermentation;
- Perform a comparative analysis between different temperature conditions and among different strains.

1.3 STRUCTURE OF THE DOCUMENT

Chapter 2 - State of the Art

Chapter 2 provides an overview of the state of the art regarding the use of dynamic GEMs in wine fermentation, including the general description of the modelling approach, plus the numerical and software tools to solve dynamic GEMs. The chapter is divided into sections to present:

1. A general overview of Systems Biology (SB);
2. A brief introduction to modelling approaches, such as FBA and dynamic flux balance analysis (dFBA);
3. A brief description of numerical tools (AMIGO2 and COBRA Toolbox);
4. A cursory state-of-the-art of the application of SB concepts to wine fermentation.

Chapter 3 - Methods

After contextualizing the relevant topics and tools for this work, a description of the methodologies is presented. First, a brief description of the latest consensus GEM of *S. cerevisiae* (Yeast8) is presented. Later in this chapter, the numerical methods required for:

1. the simulations;
2. the fluxes calculation;
3. the filtering and the assessment of the results;

are also presented.

Chapter 4 - Results and Discussion

This chapter begins with the description, and respective discussion, of the model adjustments made to portray the physiology of *S. kudriavzevii*. Later, the main results are presented and discussed. The description of the results is divided into two main sections:

1. Extracellular compounds;
2. Intracellular fluxes.

The intracellular fluxes section allows for a more detailed metabolic analysis, thus giving rise to other relevant sections:

1. Case study: block of gamma-aminobutyrate (GABA) shunt pathway;
2. Peculiar pathways/strategies of *S. kudriavzevii* CR85;
3. 25°C *versus* 12°C;
4. *S. kudriavzevii* CR85 *versus* others *Saccharomyces* strains.

Chapter 5 - Conclusion

Lastly, the Chapter 5 summarises the conclusions of the work accomplished and describes some limitations noted in the course of this work, as well as future prospects.

2

STATE OF THE ART

2.1 SYSTEMS BIOLOGY

The discovery of the structure of the deoxyribonucleic acid (DNA) molecule in the middle of XX century by Francis Crick and James Watson with the help of previous studies by Rosalind Franklin and Maurice Wilkins, is one of biology's most important breakthroughs. This groundbreaking discovery led to the development of modern molecular biology [21]. From that moment, various scientific and technological advances contributed to the genomic revolution. Today, it is possible to sequence the entire genome of organisms on an easy and inexpensive way. For example, Next Generation Sequencing (NGS) allows the analysis of the entire human genome in a single sequencing experiment, or the sequence of thousands to tens of thousands of genomes in one year.

The genomic revolution soon led to additional "omics", namely metabolomics, transcriptomics, proteomics, fluxomics, *etc*. The large volumes of data motivated a rapid growth in the field of bioinformatics. And soon, it was recognised that a more formal and mechanistic framework was needed to analyse multiple high-throughput data systematically. This need led to the application of a systems-based approach towards the study of cellular function. This multidisciplinary approximation to the cellular function study is regarded as SB [8, 22, 23].

Rather than dividing a complex problem into its parts, the systems perspective appreciates the holistic and composite characteristics of a problem and evaluates the

problem using mathematical models. From this perspective that complex behaviours emerge out of the interactions of the different biological parts, SB uses a model-based approach to study biological systems dynamics and offers the means for the control and design of biological systems [24, 25]. Hence, SB requires integrating high-throughput data (the omics data), bioinformatics and mathematical modelling, in principle, enabling the integration of data and hypotheses to predict complex interactions and behaviours. SB has the potential to be crucial in medicine (*e.g.* in deriving a mechanistic understanding of disease(s) or defining novel (personalised) treatments) or in the modern biotechnology (*e.g.* in systematic metabolic engineering, synthetic biology or food industry) [26–28].

Mathematical models tend to focus on those aspects which are relevant to address a specific biological question. Also, the modelling framework will be defined attending to the question and the available experimental data. It is out of the scope of this work to revise modelling formalisms. The interested readers can find extensive reviews elsewhere [29, 30].

Here, the focus is on the modelling of the metabolism of the cell. The metabolism includes several catabolic and anabolic pathways of enzyme-catalysed reactions that import substrates from the environment and transform them into energy and building blocks required to build the cellular components. Metabolic pathways are interconnected through intermediate metabolites, forming complex networks.

Cazzaniga et al. [31] presented a description of the computational methods available for the analysis of metabolic pathways, discussing their main advantages and drawbacks. The authors present a schematic overview of the main modelling approaches: from the coarse-grained (interaction-based, constraint based) to the fine-grained (mechanism-based) approach, and argue that modelling entails an appropriate compromise of detail. In this regard, genome-wide models, include several thousands of reactions and metabolites, while kinetic models typically focus on a few reactions.

2.2 Genome-Scale Metabolic Models

Currently, metabolic network reconstruction is a tool that has gained huge importance for the system biology of metabolism [32, 33]. The fact that full genome sequences and well-known biochemical reactions are increasingly available in several databases (Table 1) allows the extension and, consequently, generation of these metabolic networks at the genome-scale [25, 33].

Table 1: General description of databases used for the reconstruction of GEMs.

Database	Description	Website link
UniProtKB	Free access database that provides to the scientific community with high-quality data. It consists of two main sections: UniProtKB/Swiss-Prot (contains information reviewed, manually annotated); UniProtKB/TrEMBL (computationally analysed records waiting for manual annotation, unreviewed)	https://www.uniprot.org/uniprot/
BioModels	Database with mathematical models of biological and biomedical systems, which provides models published in scientific literature to the systems modelling community. It is a free access source.	https://www.ebi.ac.uk/biomodels/
NCBI	Contributes for advances in science and health with free access to biomedical and genomic information, providing access to relevant databases to biotechnology and biomedicine and it is also an important resource for bioinformatics tools and services.	https://www.ncbi.nlm.nih.gov/
KEGG	Database resource for understanding high-level functions and utilities of the biological system from molecular-level information to high-throughput experimental technologies.	https://www.genome.jp/kegg/
BRENDA	Main database to the scientific community for enzyme functional data. It is a free access database.	https://www.brenda-enzymes.org/
BioCyc	Free access microbial genome web portal which has thousands of genomes with extra information inferred by computer programs, imported from other databases and reviewed by specialized curators. It has also query tools, visualization services and analysis software.	https://biocyc.org/
GOLD	Database curated with free access to metadata for research purposes. It gives information rich resource about sequencing projects and his metadata.	https://gold.jgi.doe.gov/
SGD	Provides access to biological information, as well search and analysis tools to explore this information, that it is related to the budding yeast *Saccharomyces cerevisiae*.	https://www.yeastgenome.org/
MetaCyc	Briefly, this database contains metabolic pathways (all domains of life) that were experimentally clarified. Thus, it is a curated database.	https://metacyc.org/

Edwards & Palsson [34] presented the first GEM in 1999. According to *Gu et al.* [35], a GEM describes a full set of stoichiometry-based, mass-balanced metabolic

reactions in a biological system using gene-protein-reaction (GPR) associations that are generated from genome annotation and experimental data. A GEM can be used to predict phenotypic behaviour of the specific organism in different circumstances (genetic and environmental) or to analyse the robustness of the network [36], through optimisation-based techniques like FBA [10]. *Rocha et al.* [36] exemplify the use of GEMs to perform gene deletion analysis and integrate regulatory information.

The reconstruction of a metabolic network is an iterative and time-consuming process, and it consists of 96 steps described by *Thiele & Palsson* [33]. These steps are distributed in the following four stages: 1) draft reconstruction, 2) refinement of reconstruction, 3) conversion of reconstruction into a computable format and 4) network evaluation.

The first stage involves the genome annotation for the creation of the draft reconstruction using information available in bioinformatics databases, such the Universal Protein Resource (UniProt) [37], Kyoto Encyclopedia of Genes and Genomes (KEGG) [38] and National Center for Biotechnology Information (NCBI) [39].

The following stage involves the curation and refinement of the metabolic network by identifying biochemical reactions associated with the organism. This stage includes several steps, such as: 1) determining the GPR associations, 2) knowing the reaction directionality, 3) performing the addition of spontaneous reactions, 4) validating the reactions stoichiometry, 5) compartmentalization of identified reactions, and 6) determining the biomass composition.

The third stage is converting the network into a mathematical format to define condition-specific models that can be saved in the standard Systems Biology Markup Language (SBML) format [40].

In the last stage, also known as ”Debugging mode”, the model representation of the third stage is used to compare the organism’s behaviour prediction with experimental data, allowing an improvement of the model’s predictive potential capabilities and correctness.

Once the reconstruction becomes available, modellers can use various tools to develop genome-scale models (Table 2).

Table 2: Bioinformatic tools generally used to modelling/analysis of GEMs models.

Bioinformatic tool	Type of Software	Reference
AMIGO2	Toolbox	[19]
COBRA v.3.0	Toolbox	[20]
RAVEN 2.0	Toolbox	[41]
merlin	Standalone	[42]
CellNetAnalyser	Toolbox	[43]
Optflux	Standalone	[44]
GEMSiRV	Software	[45]

2.3 Flux Balance Analysis

The FBA is a widely used mathematical approach devoted to analysing/studying biochemical networks, especially on genome-scale metabolic models. FBA provides the flow of metabolites thought the model's network, allowing the prediction of the growth rate of a biological system or production rate of a relevant metabolite [10].

The FBA approach has a broad spectrum of use [9]. It has been applied in several complex biological challenges such as the generation of tissue-specific human metabolic reconstruction, drug discovery against pathogenic organisms and development of genetically engineered organisms for the production or not of different substances [9, 46]. The major limitations of the FBA approach are: 1) the impossibility of predicting metabolite concentrations, only fluxes can be estimated and 2) the steady-state assumption, which is only valid in particular conditions. Consequently, FBA ignores time (dynamics) and species concentrations [10, 46, 47].

2.4 Dynamic Flux Balance Analysis

The dFBA is an extension of FBA, as the name might suggest, that incorporates the rate of change of flux constraints. Therefore, it enables the prediction of external metabolites concentrations by including kinetic descriptions [11]. The dFBA approach makes the connection between steady-state intracellular metabolic flux distribution (typical FBA) with dynamic changes of environment (”new feature”) [48], allowing dynamic predictions of substrates, biomass, and product concentrations for growth in batch or fed-batch cultures [49].

2.5 Parameter estimation

Time-series experimental data describing the dynamics of the external metabolites can constrain the internal flux dynamics. The dynamics of external metabolites is described using kinetic models, and the unknown parameters can be then estimated by data-fitting.

The parameter estimation problem is formulated as an optimisation problem. The objective is to find the unknown model parameters that minimise a measure of the distance between model predictions, and the experimental data [50].

2.6 AMIGO2 Toolbox

The optimisation has a major role in multiple problems related to the modelling and design of biological systems [19]. Model identification-related problems, such as parameter estimation or optimal experimental design, may be formulated as optimisation problems, and optimisation is the underlying hypothesis in some modelling approaches (*e.g.* dFBA) [51]. Most of these problems are formulated as nonlinear programming problems (NLPs)

with dynamic and algebraic constraints. Therefore, their solution involves the use of advanced numerical simulation and optimisation methods.

AMIGO2 is multiplatform MATrix LABoratory (MATLAB) [52] based toolbox that automates the solution of such NLPs (Figure 1). The toolbox offers a series of tools devoted to the iterative identification of dynamic models, such as parameter estimation, identifiability analysis or optimal experimental design. Its dynamic optimisation module enables the use of optimality principles to predict biological behaviour or to solve multi-objective optimal control of biological systems and bioprocesses.

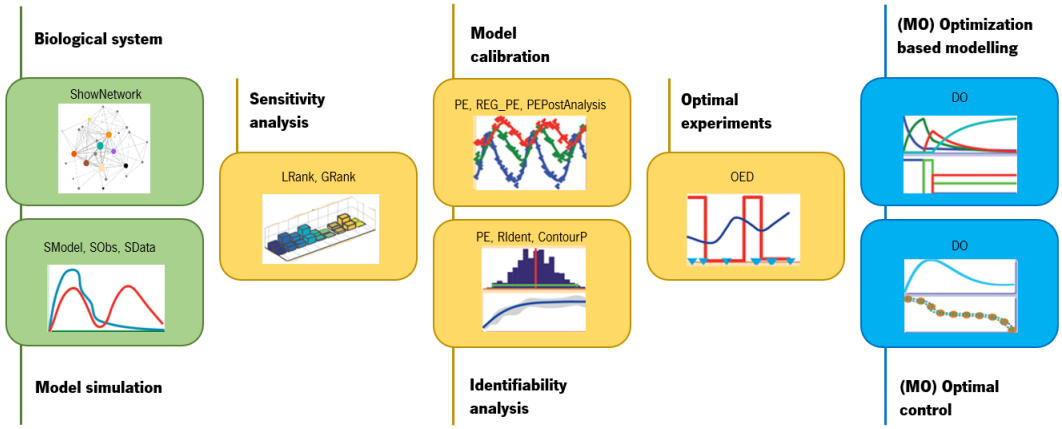

Figure 1: AMIGO2 features and tasks. Green: simulation; Yellow: sensitivity analysis; Blue: optimization. Adapted from *AMIGO2, a toolbox for dynamic modeling, optimization and control in systems biology by Balsa Canto et al., 2016. Bioinformatics, 32(21), 3358. https://doi.org/10.1093/bioinformatics/btw411* [19]

Briefly, the features of AMIGO2 will be described, according to *Balsa-Canto et al.* [19, 51]:

1. **Models:** It supports general nonlinear deterministic dynamic models and black-box simulators, dealing with ordinary, partial or delay differential equations;

2. **Experimental scheme and data:** Users can choose multi-experiment schemes with maximum flexibility and several types of Gaussian experimental noise.

3. **Parameter estimation with regularisation:** It is possible to estimate parameters and initial conditions using weighted least squares or (log-)likelihood functions. Ill-conditioned problems can be handled using the Tikhonov regularisation.

4. **Identifiability and best fit post-analysis:** The tool includes methods to analyse model identifiability: local and global parametric sensitivities; the Fisher Information Matrix for an asymptotic analysis; cost contour plots; a robust Monte-Carlo sampling approach. The χ^2 goodness of fit and Pearsons χ^2 , the autocorrelation of residuals and the Akaike and Bayesian information criteria assess the validity of models.

5. **Optimal experimental design:** AMIGO2 allows for the design of experiments oriented to improve identifiability by choosing different design objectives and experimental error descriptions.

6. **(Multi-objective) Optimal control:** Solves optimisation problems with dynamic constraints and dynamic optimisation problems (*e.g.* dFBA). For the case of multi-objective problems, the weighted sum or multi-objective optimisers can be used to obtain Pareto fronts with best trade-offs.

7. **C based enhancements:** C code is generated to enhance computational efficiency. It is possible to perform C based simulation for all available tasks; C based cost function and stand-alone C code for parameter estimation.

8. **Numerical methods:** At the simulation level, this tool incorporates the MATLAB-based initial value problem solvers and CVODES to cover stiff, non-stiff and sparse dynamic systems. Also, parametric sensitivities and exact Jacobians can be calculated. It interfaces to a set of last-generation solvers at the optimisation level to cover constrained convex and non-convex, multi-objective nonlinear optimisation problems. Users can code external optimisers in AMIGO2.

9. **Documentation:** All information needed and detailed with examples are accessible on HyperText Markup Language (HTML) documentation from the MATLAB Help menu.

In this work, AMIGO2 is used as the interface for the development of dynamic genome-scale models.

2.7 COBRA Toolbox

The so-called COBRA is a mechanistic integrative analysis framework that represents the genotype-phenotype relationship for metabolism and other cellular functions [9].

COBRA toolbox v.3.0 (latest version) is a MATLAB software package that enables quantitative prediction of cellular and multicellular biochemical networks with constraint-based modelling. Furthermore, it implements a large set of basic and advanced modelling methods as well reconstruction, model generation and model-driven analysis methods (*e.g.* variational kinetic modelling, adding biological constraints to an FBA, *etc*) [20].

Hence, COBRA toolbox can be useful for relevant research areas such as biological, biomedical and biotechnological, because it is widely used to model, analyse, and predict different kinds of metabolic phenotypes using GEMs.

2.8 Systems Biology of Wine Fermentation

This work focuses on the SB of wine fermentation. As mentioned before, modern wine production uses selected yeasts as starters to control the fermentation and confer the final product with the desired characteristics. However, the new challenges of the winemaking industry, namely: 1) the reduction of wine alcohol levels, 2) the production of distinctive

wines with improved aroma profiles and 3) the reduction of energy use, call for the benefit of new starters.

There are numerous strains of *S. cerevisiae* commercially available, but all of them generate similar ethanol yields, translating to comparable wine ethanol concentrations. Also, temperature is one of the most influential factors in the performance of fermentation and energy consumption. However, temperature reductions have widespread effects on yeast growth, and survival during fermentation [53]. Thus, commercially available *S. cerevisiae* strains are not particularly well suited to tackle industry challenges.

Initial efforts to produce low-ethanol yeasts focused primarily on generating new *S. cerevisiae* strains by genetic modification. However, considering the negative public perception and the restrictive regulations of EU toward genetically modified organisms (GMOs) in food and beverage production [54], alternatives had to be sought: adaptive evolution and hybridisation. Indeed, recent research results realised the potential of cold-tolerant species of the *Saccharomyces* genus such as *S. kudriavzevii* or *S. uvarum* to improve fermentation performance at low temperatures [7, 55–57], while reducing the final wine ethanol content.

The selection of new cold-tolerant starters requires a better knowledge of their metabolism under winemaking conditions. Very different wines can be produced from identical grapes according to the species or strain of yeast used. Hence, SB research (omics + bioinformatics + modelling) can lead to selecting new species or strains with different phenotypes, offering the winemakers with new starters to satisfy consumers' demands and improve their control over winemaking [58].

A few *Saccharomyces* non-*cerevisiae* yeasts have potential application in the winemaking industry, like *S. uvarum*, *S. kudriavzevii*, and *Saccharomyces* hybrids (*S. cerevisiae* x *S. uvarum* and *S. cerevisiae* x *S. kudriavzevii*). Several recent studies demonstrated potential advantages when fermenting at low temperatures (because of their cold-tolerant character), such as increased glycerol production, adapted membrane

composition and enhanced translation efficiency, and the capability to produce valuable aromatic compounds. Another positive sign is that these species and hybrid strains can conclude fermentation in musts with 250 g/L sugars with the customer's desirable characteristics. In addition, *S. cerevisiae* and *S. kudriavzevii* natural hybrids and the *S. kudriavzevii* can dominate industrial wine fermentation in cold climates regions and compete with *S. cerevisiae* in the earliest part of the fermentation when they are inoculated $50/50$. This dominance only happens when fermentations are conducted at low temperature [7, 56].

"Wine is not just about the grapes" because there are several features of wine-making that are dependent on the specific yeast strain choice, such as: 1) fermentation performance, 2) down-stream wine processing, 3) modulation of alcohol content and 4) levels of chemical compounds [58]. Therefore, it is crucial to have a holistic approach to SB of wine fermentation to better design novel wines.

According to *Aranda et al.* [59], thousands of yeast species are known. Still, only 15 species are considered wine yeasts and some of them are found on the surface of grapes and in the winery environment due to natural occurrences (*e.g.* wind, dispersal insects). These yeasts are part of the microflora of wine production. However, the microflora is affected by diverse meteorological or chemical factors. During the first hours of fermentation, yeasts present on the must correspond to those species found on the surface of grapes. After several hours since the beginning of the fermentation, the *Saccharomyces* yeasts dominate the fermentation (*e.g.* due to their resistance to alcohol content, the anaerobic conditions and other factors). Inoculation of the must with selected yeasts is a common practice in the wine fermentation industry, and this will drive most of the fermentation process, meaning that the yeast strain selection is a crucial step to satisfy the specifics of the final product and satisfy final costumers [58, 60].

Saccharomyces yeasts cells, the ones that stand during almost all fermentation process, have a rigid cell wall that allows them to resist the changes in osmotic pressure

and other internal characteristics that keeps them capable of doing their job. Also, the must composition is crucial for the features of the final product. The available nitrogen and carbon sources affect growth dynamics [59], since the winemaking is a batch fermentation process, generally designed as ”closed system” [61].

In recent years, various research studies focused on gaining a better understanding on how different yeast species perform during wine fermentation at multiple conditions (*e.g.* temperature, availability of sugars or assimilable nitrogen, *etc*).

Some authors explored gene expression during fermentation (*e.g.* DNA microarrays), since the desirable properties that different yeasts produce can be related, in some way, with the synthesis of specific molecules, proteins and products of enzymatic reactions [59]. Others are using complementary omics techniques.

More recently, some works address a model-based SB approach to a better process understanding and design. Modelling yeast metabolism in winemaking conditions has proved to be particularly challenging because of the grape must complexity and the dynamic nature of the process [59]. *Vargas et al.* [12] proposed using a genome-scale model, which the authors called the idFV715 model, including 1181 metabolic reactions comprising 590 components. Recently, *Henriques et al.* [15] proposed various modifications to the Yeast8 GEM (which consists of 3991 reactions and 2691 metabolites) to incorporate the lysine pathway and the production of multiple aromas pertinent to wine production. The model was solved using the dFBA approach and used to decipher the differences in the redox balance of various *Saccharomyces* species under winemaking conditions.

The potential of SB in winemaking is enormous, and further developments are to come.

3

METHODS

3.1 CONSENSUS GENOME-SCALE MODEL OF *S. cerevisiae* (YEAST8).

Yeast8, the last consensus genome-scale model of *S. cerevisiae*, is the result of an on-going iterative project devoted to building an accurate GEM for the species. Yeast4 incorporated lipid metabolism [62]; Yeast5 increased coverage, especially in sphingolipid metabolism and compatibility with COBRA toolbox [63]; Yeast6 improved the Yeast5 with additional curation, thus higher predictive accuracy of gene essentiality [64]; Yeast7 suffered a large update with a thorough revision of the representation of fatty acid, glycerolipid, and glycerophospholipid metabolism [65]. The last consensus, Yeast8, is unique because it has become a project in which everything is manually curated [17].

Nowadays, Yeast8 can be used to meet many needs of the yeast-related scientific community, and it is maintained in an open and version-controlled way (follow the project at **GitHub**). More importantly, Yeast8 gives the possibility of exploring yeast metabolism at a multi-scale level, even though it is not a dynamic GEM [17].

In this work, the extension proposed by *Henriques et al.* of the Yeast8 consensus was used as a starting point. The update includes 39 metabolites and 50 reactions needed to explore wine fermentation [15]. A further extension was implemented in this work to account for the production of erythritol and other traits of *S. kudriavzevii* CR85 in wine fermentation.

3.2 Flux Balance Analysis

This metabolic modelling approach is constraint-based, and it uses linear optimisation to determine the steady-state reaction flux distribution in a metabolic network. Hence, it requires the stoichiometric matrix (**S**) of the system to perform the steady-state analysis [47]. **S** is an $m \times n$ matrix, where each row represents one metabolite (m metabolites), and each column represents one reaction (n reactions). The stoichiometric coefficients, *i.e.* the elements of the **S** matrix, show how reactions and metabolites are related to the metabolic network. If the stoichiometric coefficient is negative, the metabolite is consumed, if it is positive, the metabolite is produced, and if the value of this metabolite is zero, it does not participate in the reaction [10]. The steady-state of the system implies that: $\mathbf{S} \times \mathbf{v} = 0$, as it is possible to see in the equation 1. However, the solution of this system of equations is not unique.

The FBA allows the computation of the flux distribution compatible with some metabolic goal given a set of flux constraints. The problem is formulated as a linear programming (LP) problem as follows:

$$\begin{aligned} &\textit{Maximize } \boldsymbol{Z} \\ &\textit{subject to}: \\ &\mathbf{S} \times \mathbf{v} = 0 \\ &\alpha_j \leq \nu_j \leq \beta_j, j = 1, \ldots N, \end{aligned} \tag{1}$$

where **v** is the vector of fluxes, α_j and β_j are the lower and upper bound of the fluxes, respectively, who reduce the space of potential solutions for the system (constraints) [36, 47]. The definition of the objective function (**Z**) is a "critical step" in FBA. Some possibilities include growth rate or adenosine triphosphate (ATP) production of the organism, among many others.

3.3 Dynamic Flux Balance Analysis

Mahadevan et al. [11] formulated dFBA in two different ways: the dynamic optimisation-based approach (DOA) and the static optimisation-based approach (SOA). In the DOA, optimisation happens during the whole period of interest to obtain time profiles of fluxes and metabolic levels. The dynamic optimisation problem is transformed into an NLP, using the so-called control vector parameterisation approach, and solved using an appropriate NLP solver. On the other hand, in the SOA, the batch time is split into multiple time intervals, and the FBA problem is solved at each time interval, for a given value of the external metabolites. In other words, the problem is solved as a succession of LP problems.

Remark that in most practical cases, the dynamic constraints describing external metabolites require the estimation of parameters by time-series data-fitting. Therefore, the DOA or SOA problems will be embedded into a nonlinear parameter estimation problem. In this scenario, the DOA approach is only doable for a reasonably low number of metabolites, while SOA (equation 2) scales better. The SOA is generally formulated as:

$$\begin{aligned}
&\underset{\mathbf{v}(t)}{Max} \quad \sum w_i v_i(t) \\
&\textit{subject to} : \mathbf{z}(t+\Delta T) \geq 0 \quad \mathbf{v}(t) \geq 0 \\
&\hat{c}(\mathbf{z}(t))\mathbf{v}(t) \leq 0 \quad \forall t \, \epsilon \, [t_0, t_f] \\
&|\mathbf{v}(t) - v(t-\Delta T)| \leq \dot{\mathbf{v}}_{max} \Delta T \quad \forall t \, \epsilon \, [t_0, t_f] \\
&\mathbf{z}(t+\Delta T) = \mathbf{z}(t) + A\mathbf{v}\Delta T \\
&X(t+\Delta T) = X(t) + \mu X(t) \Delta T,
\end{aligned} \tag{2}$$

where $\mathbf{z}$ is the vector of metabolite concentrations, X is the biomass concentration, $\mathbf{v}$ is the vector of metabolic fluxes per gram (dry weight (DW)) of the biomass, $\hat{c}(\mathbf{z}(t))\mathbf{v}(t)$ is a

vector function representing nonlinear constraints that could happen due to consideration of kinetic expressions for fluxes, *A* is the stoichiometric matrix of the metabolic network, μ is the growth rate, w_i are the amounts of the growth precursors required per gram (DW) of the biomass, t_0 and t_f are the initial and the final times, respectively, **v**(t) is the time profile of the metabolic fluxes and ΔT is the length of the time interval chosen [11].

Details on the implementation of the model considered in this work can be found in *Henriques et al.* [15, 16].

3.4 Parameter Estimation

The final model consists of 49 ODEs describing the dynamics of external metabolites. The values assigned to 82 unknown parameters (kinetic constants) will give rise to different system behaviours. The problem of parameter estimation consists of finding the unknown model parameters to minimise the distance between the model predictions and the experimental data.

From the definition it becomes apparent that the following elements are necessary to formulate the parameter identification problem: the measure of the distance among model predictions and experimental data, *i.e.* a cost function, and a suitable global optimiser to guarantee convergence to the global optimum.

As the cost function, it is selected here the weighted least squares:

$$J_{glsq}(\theta) = \sum_{d=1}^{n_d} q_d (y_d(\theta) - \widetilde{y}_d)^2 \tag{3}$$

as implemented in the AMIGO2 toolbox [50].

3.5 QUALITY OF FIT TO THE EXPERIMENTAL DATA: R^2

To quantify the quality of fit of the model the R^2 value was computed for each of the external metabolites as follows [66]:

$$R^2 = 1 - \frac{SS_{res}}{SS_{tot}} \tag{4}$$

where 1 represents the best-case scenario, *i.e.* the values of simulation totally match the experimental values, which results in SS_{res} is equal to 0 and R^2 is equal to 1. SS_{res} is the sum of squares of residuals and SS_{tot} is the total sum of squares. Hence, the R^2 value goes from 0 to 1 and the higher is R^2 value, the better, because the model explains more variability of the dependent variable.

Once R^2 values are computed for each of the 49 external metabolites, the overall quality of the model is measured using the median, ignoring negative values as they corresponded to states for which signal-to-noise ratio (SNR) is low.

3.6 NUMERICAL METHODS AND TOOLS

Solving the dFBA model requires several numerical methods. First, a method to solve ODEs (or a initial value problem (IVP) solver). Second, the optimiser to solve the FBA problem at each time step of the IVP solver, in this case, a linear programming method. Lastly, the optimiser to solve the parameter estimation problem, a non-linear programming method.

Numerical methods are selected from MATLAB [52], AMIGO2 [19] and COBRA [20] toolboxes as already mentioned in the points 6 and 7 of the chapter 2, respectively.

As for the IVP solver, *ode113* [67, 68] was used. The *ode113* is an IVP solver well suited for nonstiff ODEs that uses a time discretisation approach to solve the differential

equations. In particular, it uses a variable-step, variable-order Adams-Bashforth-Moulton solver of orders 1 to 13. At each time step, the COBRA toolbox is called to compute the optimal fluxes. Values are computed and reported back so as the dynamics of fluxes can be recovered from the initial time to final time.

As for the solution of the parameter estimation problem, the Nelder-Mead based solver *fminsearch* is used [50, 69]. The parameter estimation problem can be easily solved in AMIGO2 [19]. The scripts and data are organised and defined using AMIGO2 structures. Figure 2 presents a schematic representation of the numerical methods and tools used in the present work.

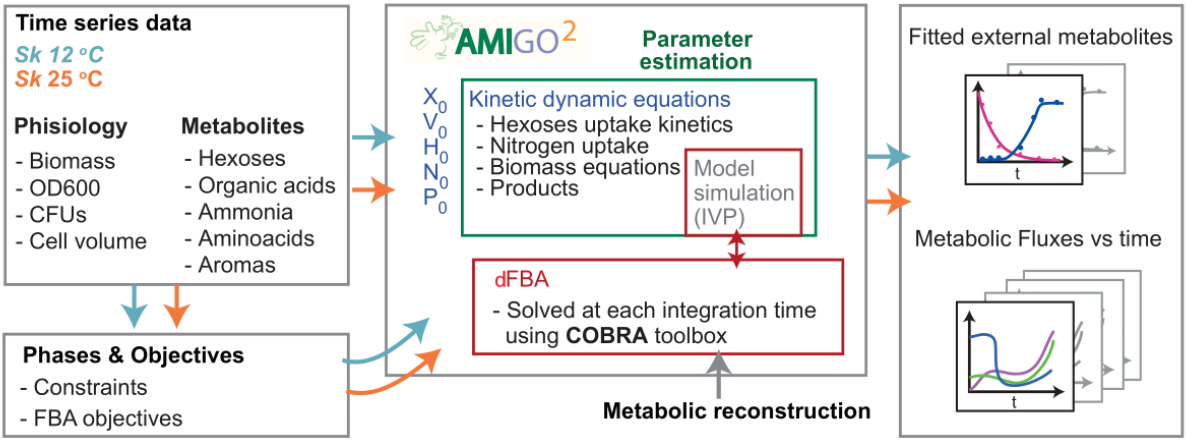

Figure 2: Scheme of combination of data and methods to solve the dFBA problem as used in this work.

3.6.1 Analysis of dynamic metabolic fluxes

The most relevant routes are selected using a score, which provides a measure of the net flux over time during growth and stationary phases for all intracellular fluxes included in the model. In particular, the integral of each flux is computed and multiplied by the biomass (mmol $\cdot$ h $^{-1}$) over time, being its value normalised by the accumulated flux of consumed hexoses (glucose and fructose):

$$S_{i,g} = 100 \cdot \frac{\int_{t_0}^{t_g} v_i(t) \cdot DW(t)}{\int_{t_0}^{t_f} v_{Glx}(t) \cdot DW(t) + \int_{t_0}^{t_f} v_{Fr}(t) \cdot DW(t)} \quad (5)$$

$$S_{i,s} = 100 \cdot \frac{\int_{t_g}^{t_f} v_i(t) \cdot DW(t)}{\int_{t_0}^{t_f} v_{Glx}(t) \cdot DW(t) + \int_{t_0}^{t_f} v_{Fr}(t) \cdot DW(t)} \quad (6)$$

where $S_{i,g}$ corresponds to the score of the flux i during growth, $S_{i,s}$ corresponds to the score during the stationary and decay phases, $v_i(t)$ (mmol $\cdot$ h $^{-1}$ $\cdot$ DW $^{-1}$) is the flux under scrutiny, $v_{Glx}(t)$ (mmol $\cdot$ h $^{-1}$ $\cdot$ DW $^{-1}$) is the flux of glucose, $v_{Fr}(t)$ (mmol $\cdot$ h $^{-1}$ $\cdot$ DW $^{-1}$) is the flux of fructose, and DW is the predicted dry-weight biomass (g). Results correspond to mmol of produced compound per mmol of consumed hexose x 100 (denoted as mmol/mmolH). Remark that the modelling is divided into two major phases: growth (from t_0 to t_g) and stationary (from t_g to t_F. Fermentation starts at $t_0 = 0$ and ends at t_F. Moreover, the multiplication by 100 of the equations 5 and 6 is to facilitate the data reading, since the original flux values are too low.

Score values indicate the overall impact of each reaction in the net oxidation or reduction of electron carriers during the given phase of the fermentation.

3.7 FILTERING OF FLUX SCORES

A total of 13318 fluxes scores are being analysed per condition and phase. All scores are organised in a matrix 13318×4. The first column collects the scores obtained at 12°C growth phase. The second, those obtained at 25°C growth phase. The third, those obtained at 12°C stationary phase and the fourth, those obtained at 25°C stationary

phase. Fluxes were filtered attending to their values, to ease the comparison between conditions and phases.

First, scores corresponding to cofactors (*e.g.* H^+, nucleotides, H_2O and others) were removed from the analysis as they are not relevant for the purpose of this work. The remaining scores in the list were filtered using MATLAB [52] with the following specification: at least one element in a row is higher than 0.1. The choice of this threshold (0.1) was *ad hoc*, since the objective of this parameter is to reduce the very low values, in order to facilitate the analysis.

The filtered matrix consists of 221 rows, *i.e.* 221 reactions. The results are organised in two excel files: the first collects scores corresponding to the growth phase and the second corresponding to the stationary phase. The reactions of each file are organised by descending order of the 25°C scores, and when the values are repeated, the order is defined by the same method for 12°C. This organisation of the scores helps to perform a better comparative analysis between different temperature conditions.

3.8 Comparative analysis of scores: Log_2 Fold Change

The comparative analysis of flux scores in the above described excel files is done by computing the relative difference between scores at 25°C and 12°C. For that purpose the log_2 fold change was computed.

Basically, the log_2 fold change of the ratio between scores at different temperatures ($S_{i,25}$ and $S_{i,12}$) were computed. If $log_2(S_{i,25}/S_{i,12}) = 1$, it would mean that the flux score at 25°C is twice the value obtained at 12°C. Similarly, if $log_2(S_{i,25}/S_{i,12)} = 2$, it would mean that the flux score at 25°C is four times the value obtained at 12°C. Conversely, if values are negative, it would imply that scores obtained at 12°C are higher. Lastly, if the

log_2 fold change is near to 0, means that there is no or very little differences between temperatures.

Reactions are considered different in those cases for which $abs(log_2) > 1$, while the reactions are assumed to behave the same for those cases for which $abs(log_2) < 1$. This classification gives an insight into which reactions, and consequent pathways, may behave differently depending on the temperature and require a detailed analysis.

4

RESULTS AND DISCUSSION

4.1 MODEL ADJUSTMENTS

As the starting point, the model proposed by *Henriques et al.* [15, 16] is used. The model consisted of a set of ODEs, describing the dynamics of the external metabolites, those consumed (sugars, nitrogen sources, O_2) and produced (alcohols, esters and carboxylic acids) plus the algebraic constraints representing the pseudo-steady metabolic state at each time step.

To adapt the dFBA model to the physiology of *S. kudriavzevii* in cold and standard temperatures, several modifications had to be introduced in the definition of the dynamics of external metabolites and the constraints on the internal fluxes. The necessary changes were introduced iteratively. For every new feature, the model was tested for qualitative and quantitative improvement.

The final version of the model proposed in the present study includes: 1) the erythritol pathway, 2) a reformulation of the model to describe acetate and alanine dynamics and 3) a redefinition of several flux constraints.

4.1.1 PRODUCTION OF ERYTHRITOL

The erythritol was the only metabolite to appear on experimental data that was not included in the previous version of the model. In order to explain its production, two reactions were added to complete the erythritol pathway, since the model already had the D-erythrose 4-phosphate metabolite [70–74].

The reactions added are:

1. **"ery"**: D-erythrose 4-phosphate [cytoplasm] $\Rightarrow$ Erythrose [cytoplasm] + Phosphate [cytoplasm];
2. **"ery2"**: Erythrose [cytoplasm] + Erythrose reductase [cytoplasm] + NADPH [cytoplasm] + H^+ [cytoplasm] $\Rightarrow$ Erythritol [cytoplasm] + $NADP^+$ [cytoplasm].

Also, the following ODE describing the production of erythritol was formulated and incorporated in the model:

$$\frac{d[Ery]}{dt} = \textbf{xdeathAndAlive} \times \left(\frac{\textbf{VEry} \times 122.12}{1000} \right) \tag{7}$$

where ***xdeathAndAlive*** represents the active cells population during the fermentation phase and the ***VEry*** is the erythritol variable, which will be multiplied by the molar mass of erythritol metabolite (122.12) and then divided by 1000 (per litre), in order to calculate the erythritol quantity per g/L. The simulation of erythritol production has to take into account the amount of active cells, hence the multiplication of these two factors. Moreover, the ID of erythritol exchange is "***EX_erythritol[c]***".

The description of the new erythritol pathway requires the addition of one parameter to the model (***pEry***). This parameter is one of the elements present in the

characterisation of the ***VEry***, which is itself described in the fermentation phases in which erythritol is present:

$$VEry = -(\textbf{vGlx} + \textbf{vF}) \times \textbf{pEry}; \tag{8}$$

where ***vGlx*** and ***vF*** are the variables of glucose and fructose that enters in the cell, respectively.

4.1.2 Reformulation of the model

The dynamics of acetate and alanine had to be adjusted at certain fermentation phases, so two model reformulations were introduced:

1. The extracellular acetate appears to be uptaken to the cytoplasm on the stationary phase of fermentation. Therefore, the bounds of acetate were reformulated as follows:

   $$\textbf{model.lb}(\textbf{rxn}) = -\textbf{ACE} \times \textbf{pAceCons} \times 1000/59.044; \tag{9}$$

   where **model.lb** is the lower bound of this reaction (**rnx**), which the ID is "***r_1634***" and represents the acetate exchange. **ACE** corresponds to acetate. This constraint is not required at the stationary phase since there is no production of acetate. The **pAceCons** is the new parameter that influences the acetate consumption. In addition, the upper bound (**model.ub**) is exactly equal to the equation 9;

2. The data shows a peak in the production of alanine in the stationary and decay phases of fermentation, thus the model equation is reformulated in these phases as follows:

   $$\textbf{vAlanine} = -\textbf{pAlaProd} \times (vGlx + vF) \tag{10}$$

where ***vAlanine*** is the variable of alanine and ***pAlaProd*** is the new parameter that helps to portray the peak of alanine to the model. The ID of alanine exchange is "***r_1873***".

4.1.3 Reformulation of flux constraints

This subsection will expose some reactions that suffered flux constraints changes, in order to achieve a more correct interpretation of *S. kudriavzevii* CR85 metabolism.

CLOSED REACTIONS. The glyoxylate cycle ("***r_0661***" and "***r_0662***") is blocked in stationary and decay stages of fermentation, because it is repressed in the presence of glucose [75] and other primary carbon sources, *i.e.* fructose and sucrose. Also, 1) the leucine precursor: 2-isopropylmalate exchange ("***r_1572***") and 2) the isoamylol precursor: 3-methylbutanal exchange ("***r_1598***") are closed as these metabolites were going to the extracellular medium without any known metabolic reason and are required to produce isoamylol in this phase.

OPENED REACTIONS. Recent studies showed that cold-tolerant strains may produce lipids in late stages of the fermentation [7, 76–78]. In order to guarantee that the model may indeed achieve such solution (if optimal) the corresponding fluxes (*e.g.* butyrate ("***r_2187***"), decanoate ("***r_1727***"), pantothenate ("***r_1548***"), mevalonate ("***r_1547***") and others) were opened.

4.2 EXTRACELLULAR COMPOUNDS

4.2.1 FIT QUALITY

The model was fit to the available experimental data. Time-series data for all external metabolites, as obtained by the IATA-CSIC at two different fermentation temperatures (12°C and 25°C), were used.

Results revealed that the model described the system dynamics successfully for both considered temperatures. The best fit to the data achieved for the biomass, amino acids and other consumed metabolites is shown in Figure 3, and for some alcohols, carboxylic acids and esters in Figure 4. The fits to the remaining external metabolites data are presented in Figures 6 and 7.

The R-squared (R^2) was determined for all measured variables and reported in each temperature figure. The vast majority of the coefficients were positive with few exceptions, typically associated with low SNR and high data dispersion observed in measured variables like cysteine, methionine, ethyl caprate, ethyl caprylate, ethyl caproate or hexyl acetate. The median of R^2 values are 0.95 for the data at 25°C and 0.87 for the data obtained at 12°C.

BIOMASS AND PHYSIOLOGICAL INDICATORS. The simulation of biomass and physiological indicators is, in general, in good agreement with the data (Figure 3.A)). Starting with colony-forming unit per Litre (CFU/L), the R^2 is 0.99 at 12°C, which corresponds to a perfect alignment with experimental data. The experimental data of CFU/L was unavailable at 25°C. The R^2 of DW/biomass is controversial, because it is -0.04 at 25°C and 0.86 at 12°C. The result obtained at 25°C can be explained by the presence of outliers in the data (see filled circles in the Figure 3.A) Biomass (g/L)). The last physiological indicator can provide a better insight of fit quality at both temperatures since the

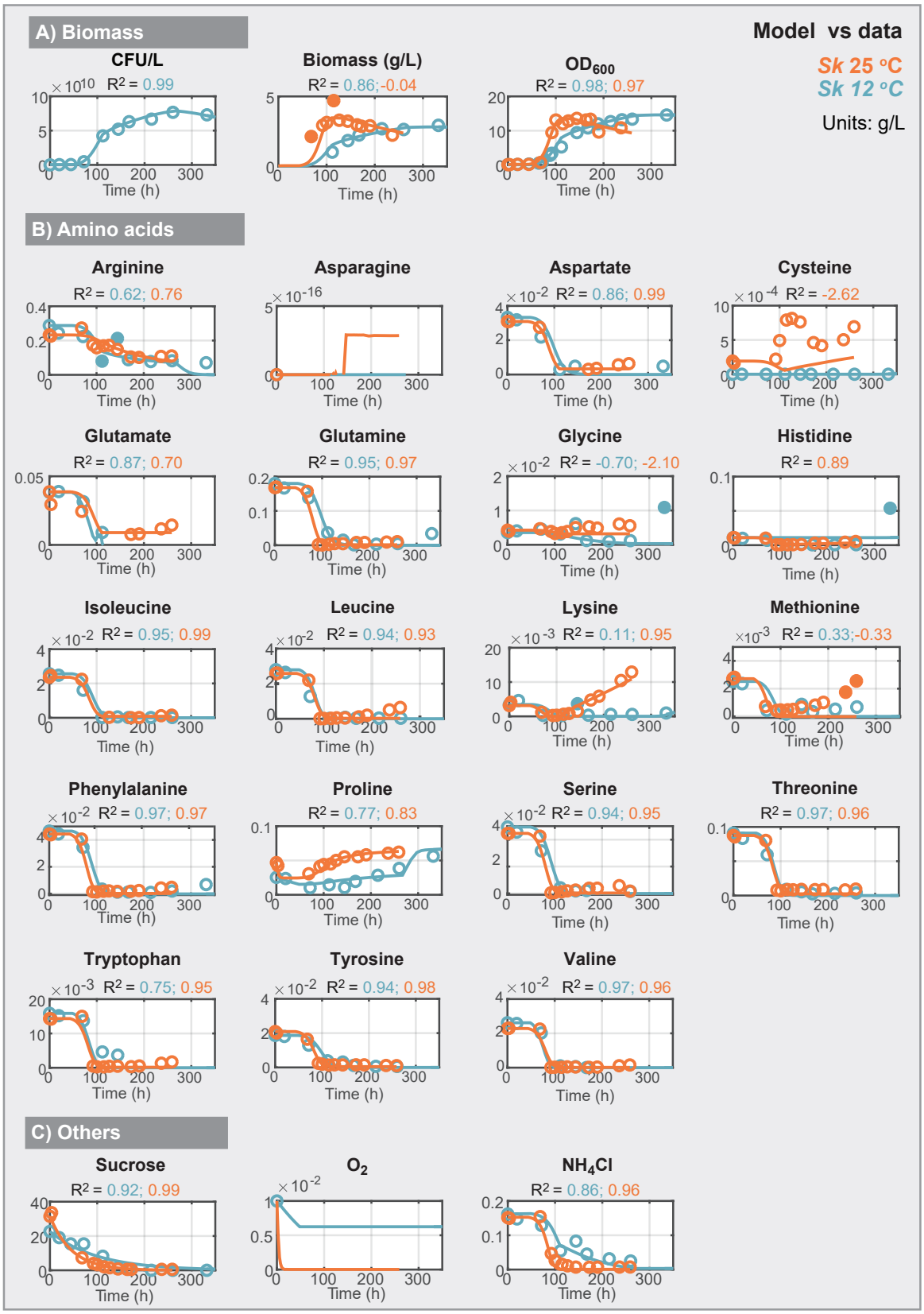

Figure 3: Plots of Model *versus* Data for: A) Biomass; B) Amino acids; C) Others consumed metabolites, are presented with their R^2 values. Lines (—): simulation; Circles (○): experimental data; Filled circles (●): outliers. Orange: 25°C; Blue: 12°C.

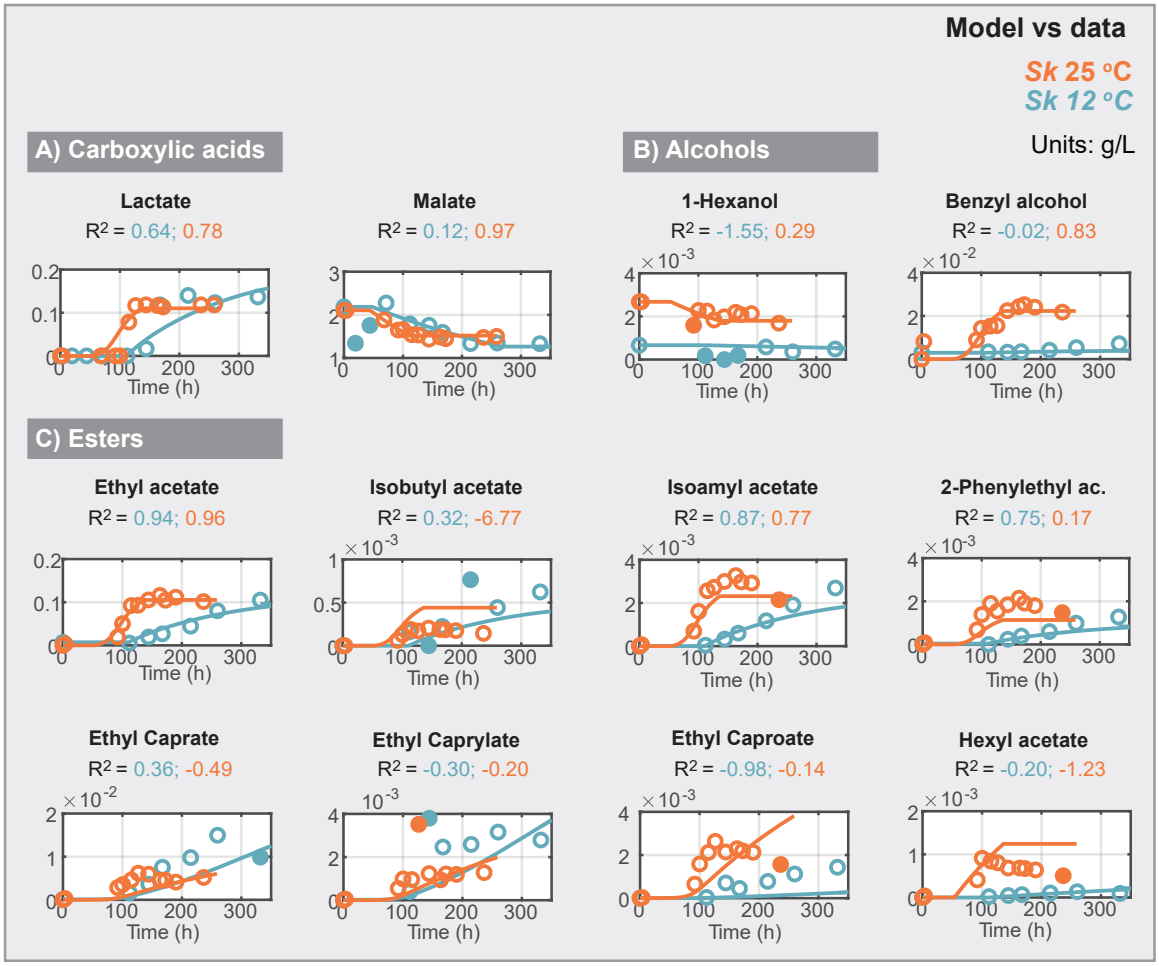

Figure 4: Plots of Model *versus* Data for: A) Carboxylic acids; B) Alcohols; C) Esters, are presented with their R^2 values. Lines (—): simulation; Circles (○): experimental data; Filled circles (●): outliers. Orange: 25°C; Blue: 12°C.

R^2 of OD600 is 0.97 at 25°C and 0.98 at 12°C. So, both simulations have an excellent R^2 value.

AMINO ACIDS. The amino acids are one of the primary sources of yeast assimilable nitrogen (YAN) compounds, while the ammonium ions are the other primary source [79]. So, it is crucial to assess the quality of the model in representing the amino acids measured. Overall, the amino acids have an excellent fit quality, with a median of R^2 above 0.9 for both temperatures (as shown in Figure 3.B)). Note that some low R^2 values are obtained for those amino acids present in very low quantities (*e.g.* methionine, cysteine, glycine) or for those with very disperse data.

HIGHER ALCOHOLS. Firstly, the main higher alcohols of this fermentation can also be distinguished by the following aliphatic alcohols (isobutanol and isoamylol) and aromatic alcohol (2-phenylethanol) terminologies. Then, the higher alcohols have a crucial role in the wine's aroma composition and are precursors of the flavour-intensive esters [80]. The R^2 values of the meaningful higher alcohols, *i.e.* 2-phenylethanol, isobutanol and isoamylol, are all higher than 0.9, which is an excellent indicator of fit quality (see Figure 7).

OTHER COMPOUNDS. Most other external compounds (*e.g.* carboxylic acids, esters and others alcohols) are present in very low amounts as can be seen in Figure 4. In those cases in which the amounts are very low and there is a substantial dispersion of the data, the model results in low R^2 values. In other cases, the R^2 values are strongly affected by the presence of outliers.

4.2.2 Duration of the fermentation phases

Fermentation duration, which differs substantially depending on the temperature, was split into five phases: lag phase, exponential growth, growth under nitrogen limitation, stationary phase and decay. The duration of the different phases was estimated during the optimisation, and the FBA problem was formulated differently in the different phases, *i.e.* either the objective or the constraints in the fluxes, or both, were changed from phase to phase (see Figure 5). Also, Figure 5, presents an overview of the general behaviour of YAN and biomass during the different fermentation phases.

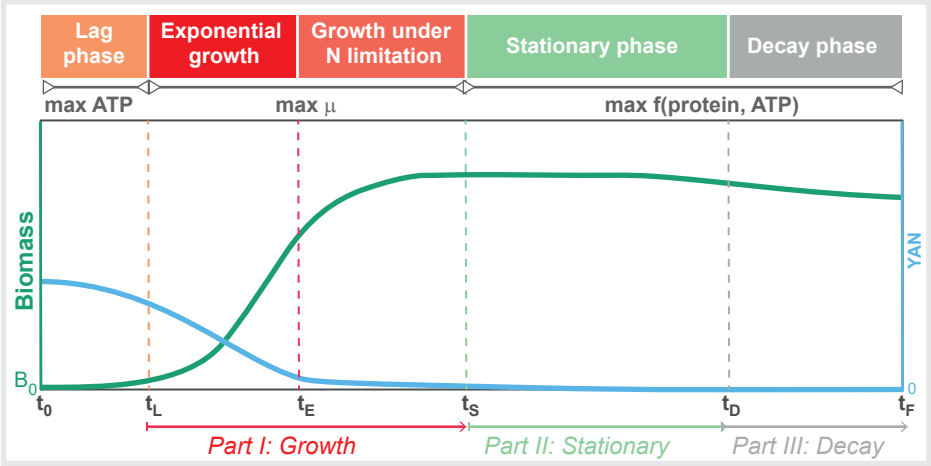

Figure 5: General representation of the fermentation phases, along with the objective function associated with each phase. Green: Biomass; Blue: YAN.

At 25°C, the lag phase lasts around 45 hours (t_L); the exponential growth lasts 9 hours (from 45 to 54 hours), the growth under nitrogen limitation phase happens between 54 (t_E) and 110 hours (t_S), the stationary phase goes until 136 hours (t_D) and the decay phase lasts until the end of fermentation ($t_F > 260$ hours). Nitrogen limitation starts at t_E, approximately, when NH_4Cl and the assimilable amino acids (YAN compounds) are lower than the actual yeast needs.

At 12°C, the dynamics are slower than that observed at 25°C. Both the lag phase and the exponential growth phases are longer: 48 hours (t_L) and 111 hours (t_E),

respectively. YAN sources are practically consumed at 267 hours (t_S), when the stationary phase starts. Decay phase starts at 390 hours (t_D) and lasts until the end of fermentation ($t_F > 500$ hours).

4.2.3 Differences in the dynamics of extracellular metabolites at 25°C and 12°C

In this subsection, the model simulations for extracellular metabolites at both temperatures are compared.

SUGARS. Sugars are consumed faster at 25°C than at 12°C. This result is in good agreement with previous studies showing that transport is affected by temperature and ethanol [15]. The transport of hexoses will vary with time, *i.e.* as soon as the cells start producing ethanol. Also, the strain does not use all fructose available in the medium at both temperatures.

AMINO ACIDS. The dynamics of uptake of amino acids seems to be independent of the temperature, exception made to the cases of lysine, alanine and proline (see Figures 3.B) and 7). The increase of lysine at 25°C, one of the first amino acids to be uptaken by yeast [81], observed at late stages of the fermentation, may be the result of cell lysis. Regarding the increase of alanine in the stationary phase at both temperatures, the intracellular fluxes simulations are presented in subsequent sections, and a plausible explanation for this behaviour is proposed.

HIGHER ALCOHOLS AND OTHER AROMAS. Higher alcohols are major volatile by-products of fermentation and can have both positive and negative impacts on wine's

aroma and flavour. Excessive concentrations of higher alcohols can result in a strong, pungent smell and taste, whereas optimal levels impart fruity characters [82].

The concentration of higher alcohols and other aromas differs at both processing temperatures. In general, the aroma production is higher at 12°C. Remarkably, final isobutanol at 12°C is more than double the amount that at 25°C (see isobutanol plot in Figure 7) and acetate at 25°C is around twice as much as at 12°C (see acetate plot in Figure 6). In addition, the nitrogen depletion could trigger the uptake of acetate, which is visible at 25°C (see Figure 6).

4.3 Intracellular fluxes

As commented in previous sections, the quality of the model in terms of its capacity of describing the dynamics of external metabolites is reasonably good. Remarkably the dFBA approach allows computing the dynamics of the internal metabolite fluxes compatible with the constraints imposed by the external metabolites plus the internal flux constraints and the cellular objectives. In the sequel, it is analysed the values obtained for the internal fluxes and, given the analysis results, it is provided a plausible explanation to the differences observed in the performance of *S. kudriavzevii* in wine fermentation at stationary phase at 12°C and 25°C.

4.3.1 Central carbon metabolism

Traditionally, the central carbon metabolism (CCM) includes the glycolysis, the tricarboxylic acid cycle (TCA cycle) and the pentose phosphate pathway (PPP). The CCM transforms carbon through these pathways to ensure energy and building blocks for cell growth and viability [83].

The Figure 6 presents the dynamics of relevant external metabolites, carbon sources and products, directly implicated in the CCM.

In winemaking conditions, the carbon flux comes from fermentable sugars *i.e.* glucose, fructose and sucrose (glucose + fructose). The model recovers quite well the dynamics of sugars: 1) $R^2 = 0.99$ at 25°C and $R^2 = 0.77$ at 12°C, for glucose, 2) $R^2 = 0.98$ at 25°C and $R^2 = 0.45$ at 12°C, for fructose and 3) $R^2 = 0.99$ at 25°C and $R^2 = 0.92$ at 12°C, for sucrose. It should be noted, that the values obtained at 12°C for both glucose and fructose can be explained taking into account that data presented an unexpected behaviour (see Figure 6).

The main product, *i.e.* ethanol, and other by-products, *i.e.* glycerol, succinate, lactate, acetate, 2,3-butanediol, erythritol, are the final destination of the majority the initial carbon skeletons present in the fermentation medium. The corresponding R^2 values are reasonably good since the majority are above 0.8. An exception is made to the succinate value at 12°C, for which the SNR is low, and data are quite dispersed.

LIPIDS AS THE MAIN DESTINATION OF CONSUMED ACETATE OF *s. kudriavzevii*. Acetate and succinate exhibit opposite directions in the cell and both have higher rates at 25°C. Regarding acetate flux ($3.95/0.12$ mmol/mmolH at 25°C and 12°C, respectively), the catabolism of this metabolite produces cytosolic acetyl-CoA which plays an important regulatory role in metabolism [84, 85]. Acetyl-CoA can be used as: 1) a substrate for the TCA cycle (it does not occur, once the carnitine shuttle is not active), 2) a precursor in the synthesis of fatty acids and steroids (the simulation suggests the mevalonate pathway as the main destination of the flux at 25°C: stoichiometry $2 \times 1.25 + 1.25$) and 3) a precursor of other anabolic pathways (production of ethyl acetate: $0.16/0.14$ mmol/mmolH at 25°C and 12°C, respectively). The simulation of the extracellular acetate showed differences between temperatures which may be explained by the use of the mevalonate pathway.

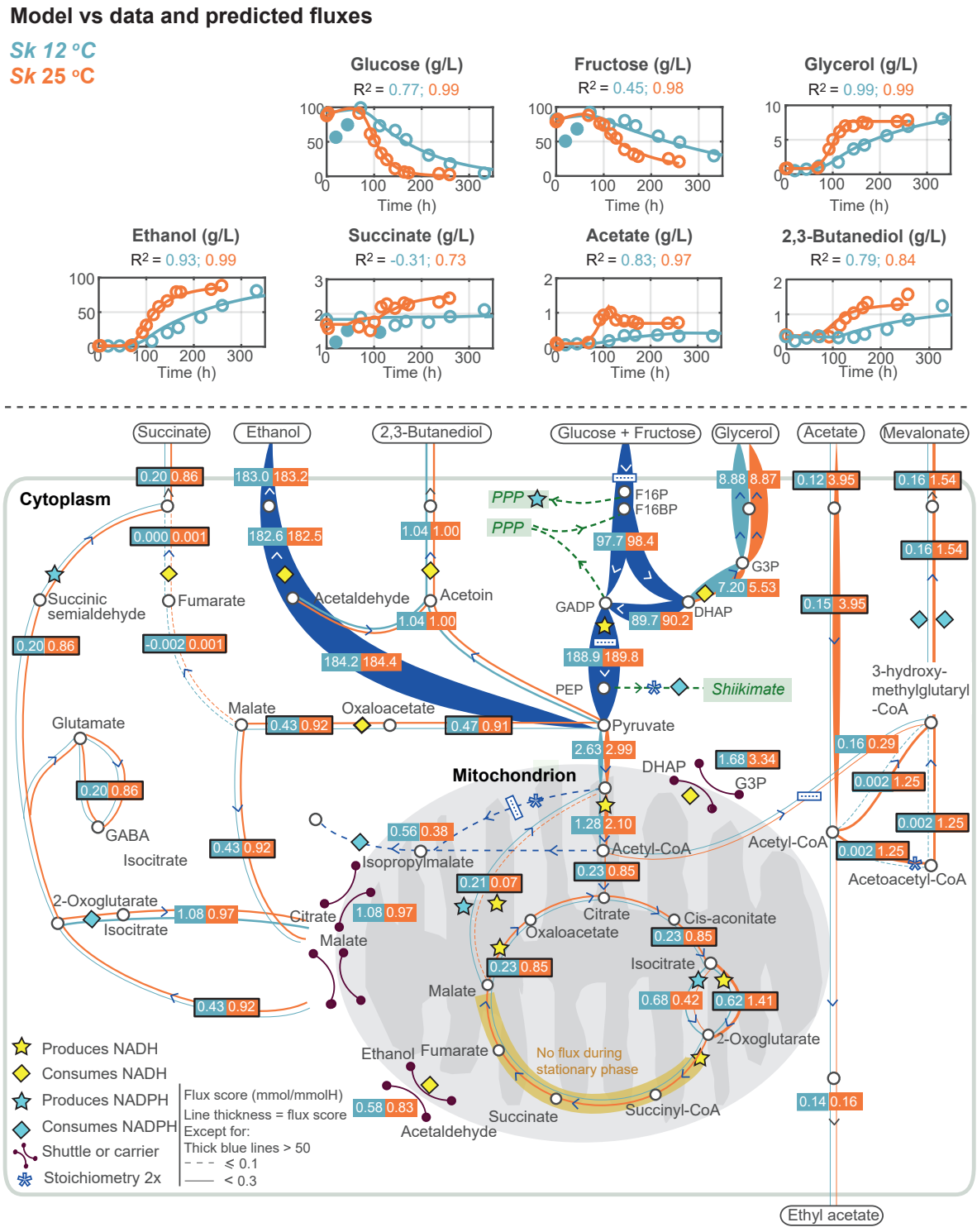

Figure 6: Central carbon metabolism, representing dynamics of sugars uptake and relevant products at the stationary phase. Plots of Model *versus* Data for sugars and relevant products are presented with their R^2 values. Orange = *S. kudriavzevii* 25°C; Blue = *S. kudriavzevii* 12°C. Lines (—): simulation; Circles (○): experimental data; Filled circles (●): outliers.

This result would confirm the hypothesis of previous works [77, 78, 86], claiming that cold-tolerant species might divert acetyl-CoA to synthesise lipids.

UNDERSTANDING SUCCINATE PRODUCTION IN THE COLD-TOLERANT YEAST SPECIES *s. kudriavzevii*. The succinate production ($0.86/0.20$ mmol/mmolH at 25°C and 12°C, respectively) comes almost entirely from the GABA shunt pathway, an alternative pathway that leads to NADPH production. Without O_2, during growth and stationary phases, the TCA cycle is truncated at the level of 2-oxoglutarate dehydrogenase and mitochondrial fumarase enzymes, which catalyse the irreversible reaction of 2-oxoglutarate to succinyl-CoA and catalyses the reversible reaction between malate and fumarate, respectively. Under such conditions, succinate can not be formed through the reductive and/or oxidative branch of the TCA cycle. Besides, malate is required to complete the oxidative branch of TCA cycle, thus malate is diverted from cytosol via the 2-oxoglutarate/malate shuttle ($0.92/0.43$ mmol/mmolH at 25°C and 12°C, respectively), basically nullifying the activity of the cytosolic fumarase enzyme. It is also important to mention that most of the malate flux that comes from the cytosol is destined to the TCA cycle at 25°C (0.85 mmol/mmolH), while nearly half of malate flux is obtained at 12°C (0.23 mmol/mmolH). The succinate production route was somehow unexpected and could be related to one of the strategies of this model to maintain the intracellular redox balance of *S. kudriavzevii* CR85.

IMPACT OF THE GABA SHUNT PATHWAY IN NADPH HOMEOSTASIS. Noticeably, the succinate production results in an NADPH accumulation (via the GABA shunt pathway), which appears to be compensated at the redox level with the mevalonate pathway (consumes NADPH) and/or vice-versa. Remarkably, simulations in this model led to a lipid biosynthesis-related pathway (mevalonate pathway) without forcing the model to do so and having the cytosolic acetyl-CoA as a precursor, in good agreement with the recent hypothesis by *Minebois et al.* [78] on the possible production of lipids. Briefly, the

model predicted that the TCA cycle does not produce succinate during the stationary phase, while the fumarase reductase has no expression in the formation of succinate. Only GABA shunt pathway produced a significant flux of succinate. The model recovers the extracellular succinate dynamics at both temperatures, and a considerable increase in succinate production can only be observed at 25°C (see Figure 6). Although previous data [76] showed substantial accumulation of intracellular GABA in cold-tolerant yeast species, the truth is that the role of the GABA shunt in yeasts is not yet well elucidated. Therefore, it was used the model to test alternative paths to succinate (see subsection 4.4).

THE TCA CYCLE DURING THE STATIONARY PHASE. The TCA cycle also shows significant differences between temperatures ($0.85/0.23$ mmol/mmolH at 25°C and 12°C, respectively). These differences originate in the fact that both TCA cycle precursors: pyruvate ($2.99/2.63$ mmol/mmolH at 25°C and 12°C, respectively) and acetyl-CoA ($2.10/1.28$ mmol/mmolH at 25°C and 12°C, respectively), have their fluxes diverted to other metabolic pathways (*e.g.* mevalonate and higher alcohols). Note that the TCA cycle does not operate as a cycle during this phase, since only a part of the oxidative branch is active.

THE TCA CYCLE OF *s. kudriavzevii* AT LOW TEMPERATURE. The flux through the TCA cycle is significantly lower at low temperatures (about 1.92 folds lower at 12°C than at 25°C). This result may be explained by the facts that: 1) part of mitochondrial pyruvate flux goes to the formation of 2-acetyllactic acid (stoichiometry $2\ \times$: $0.45/0.77$ mmol/mmolH at 25°C and 12°C, respectively), 2) part of acetyl-CoA flux goes to the formation of isopropylmalate ($0.38/0.56$ mmol/mmolH at 25°C and 12°C, respectively) and 3) another part of acetyl-CoA flux goes to the mevalonate pathway (stoichiometry $3\ \times$: $0.29/0.16$ mmol/mmolH at 25°C and 12°C, respectively). The fluxes through these alternative pathways are higher at 12°C than at 25°C, thus explaining the low

flux through the TCA cycle at 12°C. Besides, the flux towards mevalonate originates mainly via mitochondrial acetyl-CoA at 12°C and has different yields and precursors (compartmentalisation level) at different temperatures. These results further confirm the importance of the regulatory role of acetyl-CoA in metabolism.

2-OXOGLUTARATE/MALATE SHUTTLE. Still in the TCA cycle, some of the malate that was deviated from the cytosol (via 2-oxoglutarate/malate shuttle) is used to synthesise mitochondrial pyruvate ($0.07/0.21$ mmol/mmolH at 25°C and 12°C, respectively) by the malic enzyme. The regulatory pattern suggests a specific function in anaerobic metabolism, *i.e.* the provision of intramitochondrial NADPH and NADH or pyruvate [87]. However, *Boles et al.* [87] reported that under anaerobic growth conditions this specific function could be not essential, at least for *S. cerevisiae* strains in fermentations under 30°C.

GLYCEROL 3-PHOSPHATE SHUTTLE. The glycerol-3-phosphate shuttle ($3.34/1.68$ mmol/mmolH at 25°C and 12°C, respectively) presents significant differences between temperatures. This result would be in agreement with the observations by *Ansell et al.* [88], who showed that in *S. cerevisiae* strains cultured at 30°C in a defined minimal medium, anoxic conditions stimulate the mitochondrial glycerol 3-phosphate dehydrogenase. In contrast, the cytoplasmic glycerol 3-phosphate dehydrogenase was induced by osmotic stress conditions.

ETHANOL/ACETALDEHYDE SHUTTLE. The ethanol/acetaldehyde shuttle ($0.83/0.58$ mmol/mmolH at 25°C and 12°C, respectively) does not present significant differences between temperatures. Under anaerobic conditions, this shuttle can play a key role in the reoxidation of mitochondrial NADH, according to *Bakker et al.* [89], and it is visible that the TCA cycle produces a reasonable net value of NADH.

CITRATE/2-OXOGLUTARATE SHUTTLE. The citrate/2-oxoglutarate shuttle operates at both temperatures ($0.97/1.08$ mmol/mmolH at 25°C and 12°C, respectively). In the present study, this shuttle contribute to decrease of NADPH reducing power in the cytosol. On the contrary, *Castegna et al.* [90], that identified and characterised the role of this shuttle in *S. cerevisiae* at 30°C in a rich medium, affirms that the physiological role of the citrate/2-oxoglutarate carrier protein Yhm2p is to increase the NADPH reducing power in the cytosol. This difference could be caused by the fermentation conditions.

4.3.2 PENTOSE PHOSPHATE PATHWAY DURING THE STATIONARY PHASE.

Figure 7 presents the details of the PPP and the production of higher alcohols.

The Figure 7 reveals that, at stationary phase, the PPP has two operating branches: 1) the oxidative branch, producing NADPH and 2) the non-oxidative branch, producing sugars (*e.g.* fructose 6-phosphate and glyceraldehyde 3-phosphate) that will be used as intermediates for the synthesis of nucleic acids and aromatic amino acids [91]. Overall, the PPP does not present any significant differences between temperatures (see the top left side of Figure 7), but *S. kudriavzevii* CR85 simulations force all flux to go through the oxidative branch ($2.03/2.57$ mmol/mmolH at 12°C and 25°C, respectively) before entering into the non-oxidative branch. Thus, resulting in increased NADPH production.

THE PPP AS PRECURSOR OF FERMENTATION BY-PRODUCTS. The production of erythritol ($0.25/0.69$ mmol/mmolH at 25°C and 12°C, respectively) and 2-phenylethanol ($0.13/0.14$ mmol/mmolH at 25°C and 12°C, respectively) require flux through the PPP (Figure 7).

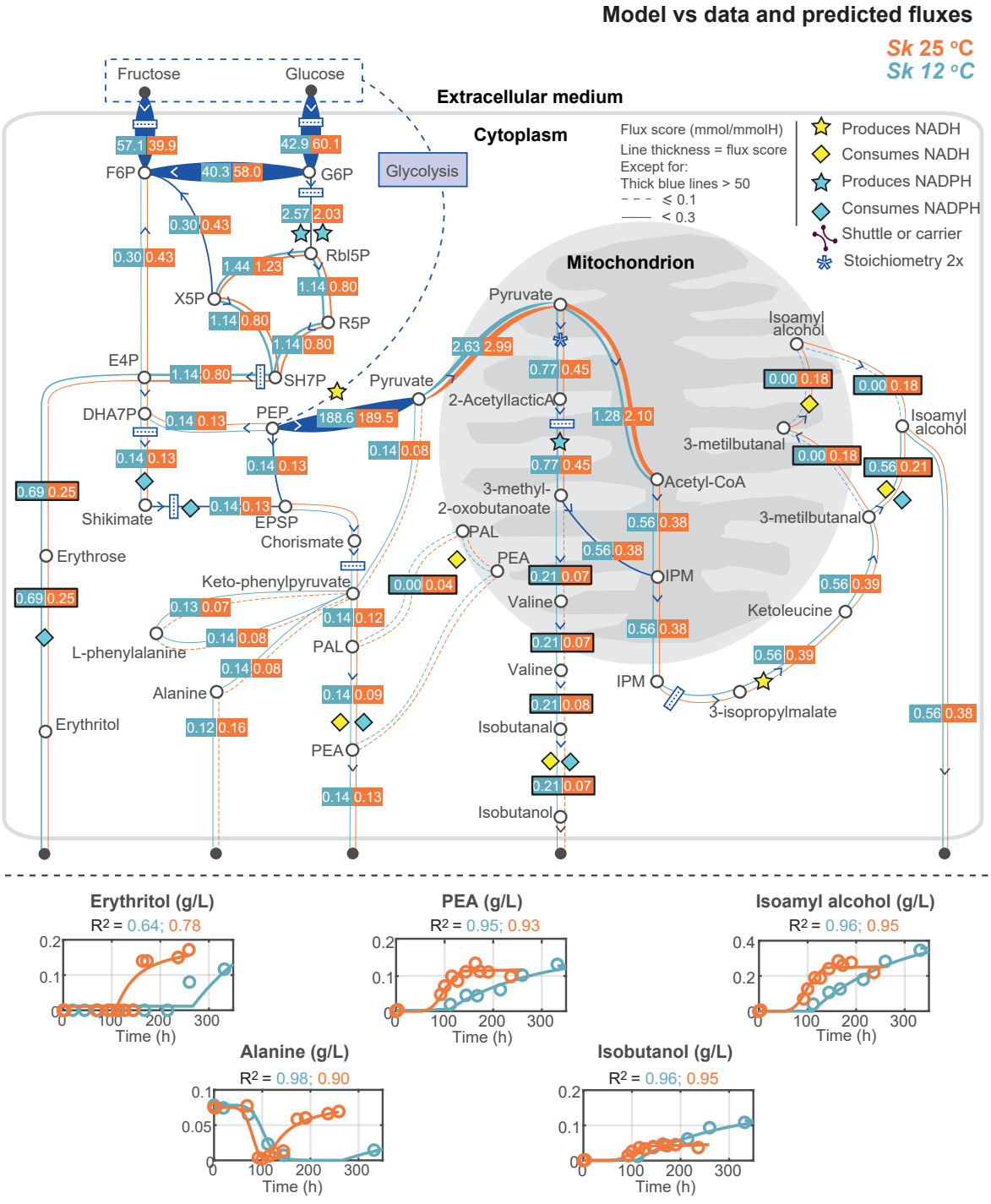

Figure 7: Production of higher alcohols, representing the dynamics of relevant products at the stationary phase. Plots of Model *versus* Data for higher alcohols and relevant products are presented with their R^2 values. Orange = *S. kudriavzevii* 25°C; Blue = *S. kudriavzevii* 12°C. Lines (—): simulation; Circles (○): experimental data; Filled circles (●): outliers.

THE IMPACT OF ERYTHRITOL PRODUCTION IN THE REDOX BALANCE AND PHYSIOLOGICAL ROLE. One unanticipated result was the production of erythritol in a significant amount at 12°C. In his review on the biotechnological production of erythritol, *Moon et al.* [72] mention the possibility of yeasts to produce erythritol. However, it had not been often found in wine production. From some possible roles, in this case erythritol may play only a role in the maintenance of redox balance (its production consumes NADPH), because the erythritol is detected in the extracellular medium. In this case, there is no evidences that it acts as osmolyte and/or storage compound. A possible explanation for the significant differences between temperatures is the fermentation conditions that at a lower temperature promotes more the production of erythritol.

4.3.3 HIGHER ALCOHOLS

The synthesis of aliphatic and aromatic alcohols is significantly influenced by the yeast strain, fermentation conditions, grape must composition, and amino acid composition [82, 92]. Their production occurs from the beginning of the growth phase to the end of the stationary phase, as shown in Figures 4.B) and 7.

EXTRACELLULAR ACCUMULATION OF ALANINE AND 2-PHENYLETHANOL. Interestingly, keto-phenylpyruvate flux (2-phenylethanol precursor) appears to participate in the biosynthesis of phenylalanine ($0.07/0.13$ mmol/mmolH at 25°C and 12°C, respectively) before contributing to the production of 2-phenylethanol. The phenylalanine degradation again produces keto-phenylpyruvate and alanine ($0.08/0.14$ mmol/mmolH at 25°C and 12°C, respectively). This process alongside with the tyrosine repeatable cycle (tyrosine degradation and biosynthesis without redox balance consequences) are the only sources of alanine (in total: $0.35/0.27$ mmol/mmolH at 25°C and 12°C, respectively) at this fermentation phase. Part of that flux will be used to supply nitrogen to the cell, and

another part is exported to the extracellular medium ($0.16/0.12$ mmol/mmolH at 25°C and 12°C, respectively). Based on previous studies with *Escherichia coli*, the synthesis of alanine at stationary phase could be related to amino acid starvation or available pyruvate concentration [93]. A possible explanation for the accumulation of extracellular alanine is the fact that alanine will not be consumed until other amino acids are completely depleted [81] and then, it is sent to the extracellular medium, because its production exceeds the required amount and only happens at a late stage of the stationary phase, in which it can begin to echo cellular death (see Alanine plot in Figure 7). Overall, this event could be related to nitrogen management strategy and do not cause any redox balance disturbance.

FLUXES ASSOCIATED WITH THE PRODUCTION OF ISOAMYLOL AND ISOBUTANOL. In mitochondria, the simulations indicate that the 2-acetyllactic acid and isopropylmalate (flux deviations of TCA cycle above-mentioned) are the metabolites that will originate the production of isoamylol and isobutanol. Firstly, the catabolism of 2-acetyllactic acid lead the formation of 3-methyl-2-oxobutanoate ($0.45/0.77$ mmol/mmolH at 25°C and 12°C, respectively) and NADPH. Part of this flux will be used ($0.38/0.56$ mmol/mmolH at 25°C and 12°C, respectively) together with acetyl-CoA to form isopropylmalate. From here, 3-methyl-2-oxobutanoate and isopropylmalate will subsequently produce final compounds, *i.e.* isobutanol and isoamylol, respectively (see Figure 7). Lastly, the production of isobutanol ($0.07/0.21$ mmol/mmolH at 25°C and 12°C, respectively) is lower than the production of isoamylol ($0.38/0.56$ mmol/mmolH at 25°C and 12°C, respectively) and presents significant differences between temperatures.

HIGHER ALCOHOLS IMPACT ON REDOX BALANCE DURING THE STATIONARY PHASE. The production of higher alcohols consume: 1) cytosolic NADPH at both temperatures and 2) mitochondrial and cytosolic NADH only at 25°C. These facts support the idea that higher alcohols production contribute substantially to the metabolic redox

balance. From the production of isobutanol and isoamylol, mitochondrial NADPH is produced (upstream of the pathways), while the production of 2-phenylethanol results in the production of cytosolic NADPH ($2\times$), oxidative branch of PPP. The NADH consumption by these compounds at 25°C could be a compensation for the alternative pathway of succinate production, since the cytosolic reductive pathway of succinate production would consume NADH and the fluxes that produce NADH are greater at 25°C, overall. There are other higher alcohols present in the intracellular fluxes simulation of fermentation, but do not present significant impact, *i.e.* methionol ($0.002/0.002$ mmol/mmolH at 25°C and 12°C, respectively) and tyrosol ($0.003/0.003$ mmol/mmolH at 25°C and 12°C, respectively), thus not shown in the Figure 7.

PRODUCTION OF HIGHER ALCOHOLS. Aliphatic and aromatic alcohols could be produced during the fermentation by two pathways: 1) Ehrlich pathway or the 2) Genevois pathway. The Ehrlich pathway is a catabolic pathway that synthesises by-products from exogenous amino acids: branched-chain amino acids (*e.g.* leucine and valine), aromatic amino acids (*e.g.* phenylalanine) and sulfur-containing amino acids (*e.g.* methionine). The Genevois pathway is an anabolic pathway, also known as the *de novo* biosynthetic pathway. The CCM provides the main carbon source for *de novo* synthesis of proteinogenic amino acids [7, 81, 94, 95]. The model predicts, that in the studies wine fermentations, higher alcohols was synthesised *de novo* since the flux routes that lead to these metabolites come from CCM, as follows in the Figures 6 and 7. This result agrees with previous results from *Crépin et al.* [96]. In their study, the authors used stable isotope tracer experiments to monitor the fate of carbon skeleton from exogenous amino acids, concluding the importance of CCM in producing higher alcohols, especially when this is the only way to synthesise them during the stationary phase.

OTHER CONSIDERATIONS. Overall, the production of higher alcohols is higher at 12°C (based on intracellular fluxes values and extracellular plots of Figure 7). Also, the

differences observed in the extracellular ethyl esters and acetate (see the Figures 4.C) and 6) lead to the conclusion that different temperatures result in different aroma profiles.

Noteworthy, cells follow the same routes to produce these compounds at different temperatures. Although, cells use some reactions (2-phenylethanol and isoamylol alcohol shuttles) to achieve redox balance only at 25°C. Isoamylol is the most produced higher alcohol and isobutanol is the only one with significant differences between temperatures, about 1.45 folds higher at 12°C than at 25°C.

4.4 Case study: Block of GABA shunt pathway

The knowledge of *S. kudriavzevii* CR85 metabolism as an alternative yeast for winemaking is still limited. The model predicted, quite surprisingly, that the GABA shunt pathway was the major contributor to succinate production. Still, it is known that succinate can also be originated through other pathways under anaerobic conditions (review *Camarasa et al.*'s article [97]).

It was tested the possibility that the GABA shunt is indeed not being used by blocking the pathway, and it was analysed the modifications observed in the metabolism.

To block GABA shunt pathway, the upper and lower bounds for the flux corresponding to the glutamate decarboxylase gene (GAD1) at stationary phase were set to zero. Again, the dFBA model was solved, the flux scores computed, and the data analysed. Results achieved in this scenario were compared to those obtained when the GABA shunt pathway was indeed active.

IMPACT ON SUCCINATE PRODUCTION. The succinate production ($0.86/0.20$ mmol/mmolH at 25°C and 12°C, respectively) still occurs in the cytoplasm, having malate and fumarate as precursors (reductive pathway) and the same flux score, *i.e.* GAD1 in-

activation does not affect succinate formation. This pathway remains with significant differences (about 2.12 folds higher at 25°C than at 12°C) and consumes NADH. The first difference between models is that instead of producing NADPH, NADH is consumed.

IMPACT ON MEVALONATE PRODUCTION. The mevalonate pathway (2.15/0.16 mmol/mmolH at 25°C and 12°C, respectively) increases its flux at 25°C, while at 12°C keeps the same flux. As a consequence, the differences between temperatures increase with respect to the previous scenario (about 3.71 folds higher at 25°C than at 12°C). Noteworthy, the mevalonate flux from mitochondria is responsible for this increase of flux at 25°C, because it increased from 0.29 (with GABA shunt pathway) to 0.90 (GABA shunt pathway blocked).

IMPACT ON THE TCA CYCLE. In mitochondria, the TCA cycle (0/0.03 mmol/mmolH at 25°C and 12°C, respectively) only works at 12°C, and the flux score is minimal.

GLYCEROL 3-PHOSPHATE SHUTTLE. Less flux is obtained through the glycerol 3-phosphate shuttle (2.34/1.21 mmol/mmolH at 25°C and 12°C, respectively), since the TCA cycle does not have too much activity.

ETHANOL/ACETALDEHYDE SHUTTLE. The ethanol/acetaldehyde shuttle (1.74/0.46 mmol/mmolH at 25°C and 12°C, respectively) presents significant differences (about 1.91 folds higher at 25°C than at 12°C). The block of GABA shunt pathway increased the flux at 25°C, while decreased the flux at 12°C, generating significant differences between temperature.

IMPACT ON HIGHER ALCOHOL PRODUCTION. The higher alcohols fluxes scores did not suffer changes with the block of GABA shunt pathway.

IMPACT ON THE PENTOSE PHOSPHATE PATHWAY. The oxidative branch of the PPP (3.38/3.16 mmol/mmolH at 25°C and 12°C, respectively) has higher flux at both temperatures, but still with no significant differences. Interestingly, with by blocking the GABA flux, the flux through the oxidative branch of PPP is higher at 25°C, since there is no GABA shunt pathway producing the NADPH required to maintain redox balance.

IMPACT ON THE 2-PHENYLETHANOL AND ERYTHRITOL. The production of 2-phenylethanol and erythritol did not suffer changes with the block of GABA shunt pathway, despite the changes observed in the oxidative branch of the PPP.

The results obtained by blocking the GABA shunt are in good agreement with previous studies by *Camarasa et al.* [97] that would suggest the reductive pathway of succinate as an alternative to the TCA to guarantee cellular viability. However, this route is sub-optimal because it is not the shortest or the most efficient solution, which keeps the GABA shunt pathway as a credible alternative. Besides, *Bach et al.* [98] reported that when grape must is rich in carbon sources, nitrogen compounds and other compounds of interest that affect growth dynamics, the GABA shunt pathway can play an important role as a source of succinate. Not to mention that this pathway is practically present in all living beings [99].

This work provided two plausible explanations for the production of succinate by this strain under these conditions. Both possibilities are compatible with the dynamics of the external metabolites. At this point, additional experimental data would be required to fully determine which is indeed the option cells use.

4.5 PECULIAR PATHWAYS/STRATEGIES OF *S. kudriavzevii* CR85

The role of this section, and respective subsections, is to summarize, consolidate and elucidate ideas of relevant pathways and strategies that occur in this model as traits in metabolism of *S. kudriavzevii* CR85 for these two temperatures.

4.5.1 MEVALONATE PATHWAY.

The mevalonate pathway generates isopentenyl pyrophosphate and dimethylallyl pyrophosphate that could be used to assemble isoprenoids. Remarkably, isoprenoids are crucial for yeast survival, since their products (*e.g.* sterols, dolichols, ubiquinones) influence several cellular processes essential for maintaining membrane integrity and viability of eukaryotic cells [100–103]. The mevalonate pathway relates to lipid biosynthesis, and the mevalonate production consumes NADPH ($2\times$), thus having a relevant impact on redox balance.

In this model, the mevalonate pathway ends with the formation of mevalonate and its export to the extracellular medium (the overall production of mevalonate comes from: 1) cytoplasm production, stoichiometry $3\ \times$: $1.25/0.002$ mmol/mmolH at 25°C and 12°C, respectively and 2) mitochondria production, stoichiometry $3\ \times$: $0.29/0.16$ mmol/mmolH at 25°C and 12°C, respectively).

Note that, mevalonate could be directed to the synthesis of lipids [86, 100]. However, it is not possible to attain such a solution without imposing specific constraints (or a cellular objective). Measurements on the production of lipids would be necessary to redirect the model solution towards the formation of lipids.

4.5.2 GABA SHUNT PATHWAY.

Basically, all living beings have the GABA shunt pathway. In yeast, this cytosolic located pathway synthesises succinate via 2-oxoglutarate, bypassing two reactions of the TCA cycle. The knowledge of its biological function appears to be limited, but *Coleman et al.* suggest that GABA shunt pathway is necessary for normal oxidative stress tolerance in *S. cerevisiae* because the GABA shunt leads to NADPH production that is critical for maintaining normal redox balance [104].

In the simulations, the GABA shunt pathway ($0.86/0.20$ mmol/mmolH at 25°C and 12°C, respectively) appearance could be related with the fact that this cold-tolerant strain is in an environmental stress situation where it is necessary to produce the NADPH required for the production of metabolites, *i.e.* erythritol and mevalonate, to protect the integrity of the cell. So, it makes sense that the succinate production happens this way. This pathway shows significant differences between temperatures (about 2.12 folds higher at 25°C than at 12°C).

4.5.3 ERYTHRITOL PATHWAY.

Erythritol, four-carbon sugar alcohol (polyol), is a naturally occurring substance widely distributed in nature. Overall, erythritol could be acting for the strain metabolism as: 1) osmolyte, 2) maintenance of redox balance and 3) storage compound, and it frequently occurs in various fruits and fermented foods (*e.g.* watermelon, grape, wine and beer) [70–72, 74]. *Liu et al.* [71] reports that erythritol production in yeast species can be triggered by excess carbon source and nitrogen starvation, and these two conditions are present in the stationary phase of the *S. kudriavzevii* CR85 at both temperatures. In this case, the erythritol formation has a role in maintaining redox balance (consumption of NADPH).

In the *S. kudriavzevii* CR85 strain, the erythritol pathway ($0.25/0.69$ mmol/mmolH at 25°C and 12°C, respectively) presents significant differences (about 1.47 folds higher at 12°C than at 25°C) and it was already detected in experimental data and mentioned in the section devoted to extracellular metabolites. The model shows that erythritol contributes to the redox balance, consuming NADPH. The conditions to produce erythritol start late in the fermentation at 12°C (see erythritol plot in Figure 7), and the fermentation lasts longer than at 25°C, as well as the conditions to its formation. This could explain why the production of erythritol is higher at 12°C than at 25°C.

4.5.4 Redox balance.

Through the analysis of the redox couples NADH/NAD^+ and NADPH/$NADP^+$ it is possible to have a perception of the redox balance strategies of the *S. kudriavzevii* CR85 strain metabolism. The NADH production is more related to catabolic processes, while NADPH is generated more frequently in anabolic pathways. However, the excess of these cofactors needs to be neutralised to achieve redox balance again and avoid reductive stress. Hence, the *S. kudriavzevii* CR85 needs to yield by-products that will consume these cofactors, but without causing oxidative stress (excessive consuming of NADH and NADPH) to the organism [105–107], because alcoholic fermentation is redox neutral under anaerobic conditions [78].

Briefly, the redox balance during the stationary phase of *S. kudriavzevii* CR85 is achieved with multiple pathways/strategies. Moreover, these pathways/strategies are basically the same at both temperatures of this study, despite some of them show significant differences between them, which will be explored in the next section. Therefore, by analysing *S. kudriavzevii* CR85 metabolism through the figures, it is possible to understand the redox balance strategies.

The NADH production is observed during: 1) glycolysis, 2) TCA cycle and 3) isoamyl alcohol pathway, while the NADH consumption occurs: 1) ethanol formation (main product of fermentation), 2) by-products production, *i.e.* glycerol and 2,3-butanediol, 3) mitochondrial shuttles, *i.e.* glycerol-3-phosphate shuttle and acetaldehyde/ethanol shuttle, 4) cytosolic malate synthesis and 5) formation of higher alcohols.

Evaluating the couple NADH/NAD^+, glycerol has relevant importance as redox valve, because its formation leads to the second major reoxidation of NADH with more impact on this fermentation phase (via glycerol biosynthesis and mitochondrial glycerol-3-phosphate shuttle). Moreover, other less common fermentative by-products, *i.e.* 2,3-butanediol [77, 97], and higher alcohols production has a little contribution to redox balance, although aliphatic and aromatic alcohols production do not consume NADH at 12°C.

Regarding the NADPH, its production is provided by: 1) the oxidative branch of PPP ($2\times$) and 2) the GABA shunt pathway, while the NADPH is required to: 1) the mevalonate pathway ($2\times$), 2) the erythritol pathway, 3) the shikimate pathway and 4) the production of higher alcohols.

Analysing the couple NADPH/$NADP^+$, the oxidative branch of PPP is the main supplier of NADPH required by the pathways mentioned above. The production of aliphatic and aromatic alcohols consumes NADPH at both temperatures, reiterating that it only consumes NADPH at 12°C.

It should be noted that *Minebois et al.* [77, 78] hypothesised that the consumption of acetate in *S. kudriavzevii* CR85 could lead to the synthesis of lipids. The model would agree with this, since the mevalonate pathway may indeed lead to the subsequent synthesis of lipids.

Remember, some authors assume that cold-tolerant strains require lipids biosynthesis to maintain the cell integrity due to the environmental stress of the medium (an increase of ethanol during fermentation) [7, 76–78]. Presumably, the GABA shunt

pathway is a redox compensation pathway that produces NADPH to maintain redox balance, since the mevalonate pathway appears as a possibility for lipid biosynthesis and consumes $2 \times$ NADPH.

4.6 25°C *versus* 12°C

Once the metabolism of *S. kudriavzevii* CR85 has been described for alternative temperature conditions during wine fermentation, it is important to understand if there are intraspecific metabolic differences between temperatures, *i.e.* which metabolic pathways differ significantly between temperatures and possible explanations. For this purpose, a comparative analysis between the different temperature conditions will be carried out, based on what has been analysed. The analysis focused on the metabolites entering and leaving the cytoplasm.

UPTAKE OF ACETATE AND MEVALONATE PATHWAY. The acetate flux uptake to the cytoplasm is significantly higher at 25°C and goes almost all to the mevalonate pathway at this temperature. The remaining flux of mevalonate is completed with flux from mitochondria without significant differences. Hence, the mevalonate flux presented a significantly higher flux score at 25°C. Following the transcriptomic and metabolic analyses of *Beltran et al.* on trying to understand the global responses of winemaking fermentations with similar temperatures, *i.e.* 25°C and 13°C, the stress responses are induced early during fermentation at low temperatures, while these adjustments are more pronounced with stationary phase at 25°C [108]. Still, this strain ability could be a survival key factor, since it could prepare the organisms to better resist environmental stresses during later fermentation phases. Similarly to the *Beltran et al.*'s work [108], the OD600 and Biomass curves (see Figure 3.A)) remain high and stable during the stationary phase at 12°C than at 25°C, where a gradual decrease is observed.

THE GABA SHUNT PATHWAY. The GABA shunt pathway produces succinate with a higher flux at 25°C. A reasonable reason for such difference is the demand of NADPH by the mevalonate pathway (consumes $2 \times$ NADPH) and has a higher flux at 25°C.

THE ERYTHRITOL PRODUCTION. The erythritol production could be a characteristic trait of this strain during wine fermentation, *i.e.* it appears not to be directly dependent of any other pathway and results of the fermentation conditions above-mentioned: 1) excess carbon source and 2) nitrogen starvation [71]. The possible explanation of erythritol has a higher flux at 12°C is the fermentation duration, because the stationary phase at 12°C lasts almost three times more than at 25°C. Hence, the conditions for the erythritol production extend further at 12°C. Incidentally, the flux score is almost three times higher at 12°C than at 25°C.

THE FLUXES INSIDE THE MITOCHONDRION. In the mitochondrion, there are significant differences between temperatures in TCA cycle, *i.e.* the flux is considerably higher at 25°C. This difference results from the cell diverting the flux to other pathways (*e.g.* mevalonate and higher alcohols). Concerning the shuttles, the glycerol-3-phosphate shuttle has higher flux at 25°C, probably because NADH production is also higher in TCA cycle, as already verified. Another plausible reason is that *S. kudriavzevii* CR85 at 25°C has difficulties in reoxidizing cytoplasm NADH, and it uses the shuttle since the stress responses are lately expressed [108]. The 2-oxoglutarate/malate shuttle significant differences are triggered by the necessity already covered of GABA shunt pathway so that the flux score will be higher at 25ºC. This same explanation is applied to cytosolic malate. Since it is at this point where more reoxidation of NADH is avoided, and malate is diverted to mitochondria. The mitochondrial malate will produce more mitochondrial pyruvate with significant differences between temperatures, thus maintaining the TCA cycle.

THE HIGHER ALCOHOLS PRODUCTION. Overall, the higher alcohols production has a better performance at 12°C, but only isobutanol presents significant differences between temperatures. This strain trait may have several reasons, it could be related to redox balance or the strain might have the natural ability to produce greater amounts of aliphatic and aromatic alcohols under low temperatures, which could be the case with the *S. kudriavzevii* CR85 and other cold-tolerant strains [92, 109]. This natural ability could be also a consequence of higher viability of the cells during lower temperatures [108], therefore increasing the production of higher alcohols during the stationary phase. Lastly, the higher alcohols production consumes cytosol and mitochondrial NADH only at 25°C.

Briefly, the *S. kudriavzevii* CR85 metabolism has different behaviours at different temperatures since there are a set of reactions where significant differences between temperatures are identifiable. Basically, the pathways are the same at both temperatures. Hence, the Table 3 provides a widespread approach of the pathways where the strain makes the adjustments at this fermentation phase.

Table 3: The reaction(s) and respective pathways responsible for the main differences between temperatures with the Log_2 Fold Change and temperature with the highest flux score are displayed at stationary phase. The reactions cofactors are ommited for a better visualization. **Legend**: **[e]** = extracellular medium; **[c]** = cytoplasm; **[m]** = mitochondria; ⇒ = reaction direction; **[...]** = pathway shorcut. **Abbreviations**: **HMG-CoA** = 3-hydroxy-3-methylglutaryl-CoA; **E4P** = Erythrose 4-phosphate; **DHAP** = Dihydroxyacetone phosphate; **GP3** = Glycerol 3-phosphate.

Reaction(s)	Pathway(s)	Log_2 Fold Change	Higher at:
Acetate [c] ⇒ Acetyl-CoA [c]	Acetate utilization	4.72	25°C
HMG-CoA [c] ⇒ Mevalonate [c] ⇒ [e]	Mevalonate pathway	3.23	25°C
GABA [c] ⇒ Glutamate [c] ⇒ Succinate [c] ⇒ [e]	GABA shunt pathway	2.12	25°C
E4P [c] ⇒ Erythrose [c] ⇒ Erythritol [c] ⇒ [e]	Erythritol pathway	1.47	12°C
Isobutanal [c] ⇒ Isobutanol [c] ⇒ [e]	Valine degradation	1.66	12°C
Acetyl-CoA [m] ⇒ Citrate [m] ⇒ [...]	TCA cycle	1.92	25°C
DHAP [m] ⇒ G3P [m] ⇒ G3P [c]	Glycerol 3-phosphate shuttle	1.68	25°C
Oxaloacetate [c] ⇒ Malate [c] ⇒ Malate [m]	2-oxoglutarate/Malate shuttle	1.08	25°C
Malate [m] ⇒ Pyruvate [m]	TCA cycle	1.61	12°C

4.7 *S. kudriavzevii* CR85 *versus* OTHER *Saccharomyces* STRAINS

The comparison of the metabolism of *S. kudriavzevii* CR85 with that of other *Saccharomyces* strains can give a better insight of the fermentative potential of this yeast under alternative temperatures. Here, the comparison is performed using recent results (unpublished) obtained by *Henriques et al.* for three yeasts strains (*S. cerevisiae* T73 (T73), *S. uvarum* BMV58 (SuB) and *S. uvarum* CECT12600 (SuC)) at 25°C.

Noteworthy, this brief comparative analysis will be approached in two main topics: 1) metabolic pathways differences and 2) analysis of metabolite fluxes, and limited to the stationary phase, since it is the main focus of the work.

A set of differences is observed when comparing the metabolic pathways of *S. kudriavzevii* CR85 simulations *vs* other *Saccharomyces* yeasts. The Table 4 presents some relevant reactions, related to the CCM and the production of higher alcohols, which being present in the fermentations performed with one strain were not present in the others.

Table 4: Metabolic pathways differences of five different fermentative profiles at stationary phase. The pathways are related with CCM and higher alcohols production. X: non active; ✓: active. **Abbreviations: Sk** = *S. kudriavzevii*.

Pathway(s)	**Reactions's ID**	**T73**	**SuB**	**SuC**	**Sk 25°C**	**Sk 12°C**
Mevalonate pathway	r_0559	X	✓	✓	✓	✓
Carnitine shuttle	r_0254	X	✓	✓	X	X
Succinate (GABA shunt pathway)	r_0469	✓	✓	✓	✓	✓
Succinate (cytosolic reductive pathway)	r_1000	X	✓	✓	X	X
Erythritol pathway	ery	X	X	X	✓	✓
Alanine transport (to extracellular medium)	r_1183	X	X	X	✓	✓
PPP (all flux through oxidative branch)	r_1050/ r_1040	X	X	X	✓	✓
2-phenylethanol (shuttle)	r_0170	✓	✓	✓	✓	X
Isoamylol alcohol (shuttle)	r_0180	✓	✓	✓	✓	X

THE PRODUCTION OF LIPIDS. Both the cold-tolerant species *S. uvarum* and *S. kudriavzevii* produced mevalonate (lipid related pathway), while *S. cerevisiae* T73 does not divert any flux towards mevalonate at stationary phase.

THE SUCCINATE PATHWAYS. As mentioned before, there are two different pathways to succinate formation: 1) via GABA shunt pathway and 2) via cytosolic reductive pathway. The results indicate that all yeasts produce succinate via GABA shunt pathway, while only *S. uvarum* strains use both pathways to produce succinate.

s. kudriavzevii CR85 TRAITS. The *S. kudriavzevii* CR85 presents a clearly differential behaviour for some particular pathways, comparing with the other strains. The production of erythritol is not a surprise, since it was necessary to include the reactions to this model for this yeast. The alanine increase of extracellular medium also required a reformulation to the model. Lastly, the PPP of *S. kudriavzevii* CR85 forces all flux through the oxidative branch before entering into the non-oxidative branch, since the two reactions (regulated by transketolases enzymes) have reverse directions. The other yeasts have, at least, one of the reactions with the normal direction to non-oxidative branch, by-passing the oxidative branch.

THE SHUTTLES DIFFERENCES. From these five different fermentative profiles, *S. uvarum* strains are the only yeasts having flux through the carnitine shuttle and the *S. kudriavzevii* CR85 at 12°C is the only fermentative profile that does not have flux through the shuttle of 2-phenylethanol and isoamylol alcohol.

In the sequel, the fermentation profiles are further analysed to explore quantitative differences. The Table 5 show the fluxes corresponding to relevant reactions which are related to CCM and the production of higher alcohols.

Table 5: Comparative analysis of five different fermentative profiles at stationary phase. The reactions are related with CCM and higher alcohols production. **Legend: [e]** = extracellular medium; **[c]** = cytoplasm; **[m]** = mitochondria; ⇒ = reaction direction. **Abbreviations: Sk** = *S. kudriavzevii*.

Reactions	T73	SuB	SuC	Sk 25°C	Sk 12°C
Ethanol [c] ⇒ [e]	187.33	179.14	184.24	183.2	183
Glycerol [c] ⇒ [e]	7.09	7.84	7.81	8.87	8.88
Succinate [c] ⇒ [e]	0.43	6.08	1.66	0.86	0.2
2,3-butanediol [c] ⇒ [e]	0.17	0.54	0.85	1	1.04
Ethyl acetate [c] ⇒ [e]	0.15	0.17	0.19	0.16	0.14
Acetate [e] ⇒ [c]	0	0.47	0.71	3.95	0.12
Mevalonate [c] ⇒ [e]	0	0.07	0.04	1.54	0.16
Pyruvate [c] ⇒ [m]	3.22	3.64	2.34	2.99	2.63
Acetyl-CoA [m] ⇒ TCA cycle	0.49	2.07	1.40	0.85	0.23
Acetyl-CoA [m] ⇒ Isopropylmalate [m]	0.87	0.5	0.41	0.38	0.56
Pyruvate [m] ⇒ 2-acetyllactic acid [m]	0.97	0.59	0.5	0.45	0.77
Isoamylol alcohol [c] ⇒ [e]	0.74	0.48	0.39	0.38	0.56
Isobutanol [c] ⇒ [e]	0.1	0.08	0.08	0.07	0.21
2-phenylethanol [c] ⇒ [e]	0.16	0.66	0.38	0.13	0.14

PRODUCTION OF MAIN PRODUCTS. Overall, the T73 produces more ethanol and less others main by-products than the others yeasts. Other remarkable points: 1) the *S. kudriavzevii* CR85 produces more glycerol and 2,3-butanediol at both temperatures, 2) succinate is highly produced by SuB (6.08 mmol/mmolH) and SuC (1.66 mmol/mmolH), correlated to the existence of two vias of succinate production, while the *S. kudriavzevii* CR85 produces a little amount at 12°C (0.2 mmol/mmolH), comparing to the other strains.

UPTAKE OF ACETATE. The acetate uptake does not occurs in the T73, but occurs on the other yeasts with special attention for *S. kudriavzevii* at 25°C (3.95 mmol/mmolH), where the amount of uptake is large relatively to the others profiles. This event are related with the mevalonate formation.

THE MEVALONATE PATHWAY. This lipid related pathway appears only in simulation of the alternative yeasts to wine fermentation (*S. uvarum* and *S. kudriavzevii*). High-

light, the highly amount of flux of S. kudriavzevii at 25°C (1.54 mmol/mmolH), taking in consideration the other profiles and the respective acetate uptakes.

THE FLUXES OF MITOCHONDRIA. Despite of the flux that enters in the mitochondria does not be present notable differences, it is possible affirm that the *S. uvarum* species have more activity on the TCA cycle (2.07 mmol/mmolH for SuB and 1.4 mmol/mmolH for SuC) than the other profiles, while the T73 has more flux towards the branched-chain amino acids (BCAAs) and higher alcohols production (isopropylmalate: 0.87 mmol/mmolH and 2-acetyllactic acid: 0.97 mmol/mmolH).

FORMATION OF HIGHER ALCOHOLS. The fact that T73 has more flux to BCAAs and higher alcohols production results in the higher production of isoamylol alcohol of all strains. The isobutanol has a minimal production, exception made for the *S. kudriavzevii* at 12°C (0.21 mmol/mmolH) and the SuB (does not produce). The 2-phenylethanol production is significantly higher in the *S. uvarum* strains.

Firstly, these differences (see Table 4) could be related with different redox homeostasis strategies of the strains, as discussed in the *S. kudriavzevii* under alternative temperatures. Hence, others reasons for these differences are the environmental stresses and/or peculiar traits of strains.

In these results, the *S. kudriavzevii* fermentation profile could have some desirable advantages as alternative fermentative yeasts. Results shown in Table 5 confirm that fermentations started with *S. kudriavzevii* are suited to achieve consumers demands: 1) lower production of ethanol than T73 and SuC, 2) higher production of glycerol than all others strains, providing a wine with more sweetness [110], 3) higher production of 2,3-butanediol than all others strains, which is associated with a desirable flavour [82, 111], 4) a reasonable production of succinate (lower to that produced by *S. uvarum* strains), which is positive, since succinate has an ”unusual salty, bitter taste” [82] and 5)

a unique performance of higher alcohols that together with acetate and the production of ethyl esters could originate a different aroma profile.

Conversely, there are some disadvantages: 1) the time required to reach the end of fermentation is larger than for other species and 2) the production of 2-phenylethanol - which contributes to the fruity and floral aromas of the wine [92]- is lower than the production by *S. cerevisiae*.

5

CONCLUSION

5.1 FINAL CONSIDERATIONS

The successful formulation of dynamic constraints, *i.e.* new erythritol's ODE, model reformulations, flux constraints reformulations, led to an updated model capable of simulating the dynamics of the metabolism of *S. kudriavzevii* CR85 under wine fermentation conditions, throughout the AMIGO2 toolbox [19] and its interface with COBRA toolbox [20].

This model is highly capable of explaining the metabolism of *S. kudriavzevii* CR85 under different fermentation temperatures, as confirmed by the median R^2 values of 0.95 and 0.87 at 25°C and 12°C, respectively. Moreover, biomass measures, carbon sources and the main by-products also have good R^2 values.

Through the metabolic description focused on the stationary phase for alternative temperature conditions during the wine fermentation, some points are highlighted:

1. Lipids are the main destination of uptaken acetate at 25°C. This cold-tolerant species requires acetyl-CoA (cytoplasmic + mitochondrial) to produce lipids, as already hypothesised in other studies [77, 78, 86];

2. Succinate production comes via GABA shunt pathway, also known as an alternative pathway for succinate formation. This pathway appears to supply the NADPH needs of strain, since the mevalonate production consumes NADPH;

3. The production of erythritol could be associated with cold-tolerant strains, because of its possible role in the maintenance of redox balance [72] and the duration of fermentation (characteristic of low temperatures fermentations [112]);

4. Overall, the performance of aliphatic and aromatic alcohols is higher at 12°C, which could be caused by the viability of the strain to extend over time at low temperatures [108], increasing their production during the late fermentation phases.

After that, some metabolic differences between temperatures were observed:

1. The mevalonate pathway has a significant higher production at 25°C than at 12°C. According to *Beltran et al.* [108], during wine fermentation at 25°C this general stress response appears to be more related with the stationary phase, while at lower temperatures this stress response is induced early [108];

2. The production of succinate also differs between different temperatures (25°C $>$ 12°C). This difference may be a consequence of the lipids production (redox balance maintenance);

3. Erythritol has a production significantly higher at 12°C than at 25°C, since the conditions for its production: 1) excess carbon source and 2) nitrogen starvation [71] extend longer at 12°C;

4. The only higher alcohol with significant differences is isobutanol (12°C $>$ 25°C);

5. The aromatic profiles from both temperatures have some differences, since the production of higher alcohols is higher at 12°C. The extracellular acetate is higher at 25°C (see acetate plot of Figure 6), and most esters accumulate higher amounts at 25°C (see esters plots of Figure 4.C)).

Overall, the analysis of *S. kudriavzevii* CR85 metabolism allows to affirm the capacity of winemaking at alternative temperatures without compromising any of the fermentation phases, *i.e.* the fermentation occurs without disruptive events. In addition,

the Table 5 allows to perspective some potential advantages of *S. kudriavzevii* CR85 relatively to other *Saccharomyces* strains.

5.2 Difficulties and limitations

In this section, a number of difficulties and limitations faced during the development of this project are summarised:

1. The amount of data is significantly larger to the data available in previous modelling exercises, counting on time-series data for dozens of extracellular components. However, it would be desirable to count on more data specifically on lipids, which it would help to explore further the role of mevalonate;

2. Computational effort for parameter estimation is quite substantial. In this regard, the use of a personal computer limited the possibility of using advanced global optimisers and uncertainty analyses;

3. The COVID-19 pandemic and the lock-down situation in Spain and the measures adopted at the host institution (IIM-CSIC) forced that all discussions and exchange of ideas had to be on-line. This was not ideal, but it worked reasonably well.

5.3 Future works

As mentioned before, modelling yeast metabolism under enological conditions is an iterative and demanding process, because of the grape must complexity and the dynamic nature of the process [59]. With the possibility of multi-omics data and novel computational methods, there is always space to improve this model.

Among other possible improvements, some further explorations are suggested:

1. The mevalonate pathway ends in the mevalonate, which is a middle step of the pathway that will produce precursors that could be used to assemble isoprenoids [100]. So, new data will provide the means to specify new constraints to decipher the role of lipids as reducing equivalents;

2. Further transcriptomic and metabolic experiments are recommended, in order to understand more accurately how succinate is produced in *S. kudriavzevii* CR85 under alternative temperature conditions during the wine fermentation;

3. A global metabolic approach, *i.e.* the analysis of further fermentation phases, would provide a better metabolic knowledge of the strain during winemaking;

4. Perform a more thorough comparative analysis between different strains of the *Saccharomyces* genus, accounting for both extracellular and intracellular fluxes, in order to better assess the potential of cold-tolerant strains as alternative starters for the winemaking industry.

BIBLIOGRAPHY

[1] Soleas, G. J., Diamandis, E. P., & Goldberg, D. M. (1997). Wine as a biological fluid: History, production, and role in disease prevention. *Journal of Clinical Laboratory Analysis*, *11*(5), 287–313.

[2] International Organisation of Vine and Wine (OIV). (2019). *State of the vitiviniculture world market - state of the sector in 2018* (tech. rep. No. 4).

[3] Wine market observatory. (2019). Retrieved November 26, 2019, from https://ec.europa.eu/info/food-farming-fisheries/farming/facts-and-figures/markets/overviews/market-observatories/wine_en#marketdata_dashboard

[4] OIV - State of Vitiviniculture. (n.d.). Retrieved November 26, 2019, from http://www.oiv.int/en/technical-standards-and-documents/statistical-analysis/state-of-vitiviniculture#Conditionsreport

[5] Mozell, M. R., & Thach, L. (2014). The impact of climate change on the global wine industry: Challenges & solutions. *Wine Economics and Policy*, *3*(2), 81–89.

[6] White, M. A., Diffenbaugh, N., Jones, G. V., Pal, J., & Giorgi, F. (2006). Extreme heat reduces and shifts united states premium wine production in the 21st century. *Proceedings of the National Academy of Sciences*, *103*(30), 11217–11222.

[7] Pérez-Torrado, R., Barrio, E., & Querol, A. (2018). Alternative yeasts for winemaking: *Saccharomyces* non-*cerevisiae* and its hybrids. *Critical Reviews in Food Science and Nutrition*, *58*(11), 1780–1790.

[8] Kitano, H. (2001). *Foundations of Systems Biology*. The MIT Press Cambridge, Massachusetts London, England.

[9] Palsson, B. Ø. (2015). *Systems Biology: Constraint-based reconstruction and analysis*. Cambridge University Press.

[10] Orth, J. D., Thiele, I., & Palsson, B. Ø. (2010). What is flux balance analysis? *Nature Biotechnology*, *28*(3), 245–248.

[11] Mahadevan, R., Edwards, J. S., & Doyle III, F. J. (2002). Dynamic flux balance analysis of diauxic growth in *Escherichia coli*. *Biophysical Journal*, *83*(3), 1331–1340.

[12] Vargas, F. A., Pizarro, F., Pérez-Correa, J. R., & Agosin, E. (2011). Expanding a dynamic flux balance model of yeast fermentation to genome-scale. *BMC Systems Biology*, *5*(1), 75.

[13] Sánchez, B. J., Pérez-Correa, J. R., & Agosin, E. (2014). Construction of robust dynamic genome-scale metabolic model structures of *Saccharomyces cerevisiae* through iterative re-parameterization. *Metabolic Engineering*, *25*, 159–173.

[14] Förster, J., Famili, I., Fu, P., Palsson, B. Ø., & Nielsen, J. (2003). Genome-scale reconstruction of the saccharomyces cerevisiae metabolic network. *Genome Research*, *13*(2), 244–253.

[15] Henriques, D., Alonso-del-Real, J., Querol, A., & Balsa-Canto, E. (2018). *Saccharomyces cerevisiae* and *S. kudriavzevii* synthetic wine fermentation performance dissected by predictive modeling. *Frontiers in Microbiology*, *9*, 88.

[16] Henriques, D., Minebois, R., Pérez-Torrado, R., Balsa-Canto, E., & Querol, A. (2018). Multi-scale modeling to explain wine fermentation. In *FOODSIM'2018* (pp. 259–263). Univ. Leuvre, Ghent, Belgium.

[17] Lu, H., Li, F., Sánchez, B. J., Zhu, Z., Li, G., Domenzain, I., ... Lieven, C. et al. (2019). A consensus *S. cerevisiae* metabolic model Yeast8 and its ecosystem for comprehensively probing cellular metabolism. *Nature Communications*, *10*(1), 1–13.

[18] Lewis, N. E., Hixson, K. K., Conrad, T. M., Lerman, J. A., Charusanti, P., Polpitiya, A. D., ... Palsson, B. Ø. (2010). Omic data from evolved *E. coli* are consistent with computed optimal growth from genome-scale models. *Mol. Syst. Biol*, *6*(1), 390.

[19] Balsa-Canto, E., Henriques, D., Gábor, A., & Banga, J. R. (2016a). AMIGO2, a toolbox for dynamic modeling, optimization and control in systems biology. *Bioinformatics*, *32*(21), 3357–3359.

[20] Heirendt, L., Arreckx, S., Pfau, T., Mendoza, S. N., Richelle, A., Heinken, A., ... Vlasov, V. et al. (2019). Creation and analysis of biochemical constraint-based models using the COBRA Toolbox v. 3.0. *Nature Protocols*, *14*(3), 639–702.

[21] Klug, A. (2004). The discovery of the DNA double helix. *DNA: Changing Science and Society*, *17*, 5.

[22] Westerhoff, H. V., & Palsson, B. Ø. (2004). The evolution of molecular biology into systems biology. *Nature Biotechnology*, *22*(10), 1249–1252.

[23] Mardis, E. R. (2008). The impact of next-generation sequencing technology on genetics. *Trends in Genetics*, *24*(3), 133–141.

[24] Kitano, H. (2002). Systems Biology: a brief overview. *Science*, *295*(5560), 1662–1664.

[25] Dias, O. (2013). *Reconstruction of the genome-scale metabolic network of Kluyveromyces lactis* (Doctoral dissertation, Dept. BioEng., Minho Univ., Braga).

[26] Antoranz, A., Sakellaropoulos, T., Saez-Rodriguez, J., & Alexopoulos, L. G. (2017). Mechanism-based biomarker discovery. *Drug Discovery Today*, *22*(8), 1209–1215.

[27] Benner, S. A., & Sismour, A. M. (2005). Synthetic biology. *Nature Reviews Genetics*, *6*(7), 533–543.

[28] Schmitz, U., & Wolkenhauer, O. (2016). *Systems medicine*. Springer.

[29] Machado, D., Costa, R., Rocha, M., Ferreira, E., Tidor, B., & Rocha, I. (2011). Modeling formalisms in systems biology. *AMB Express*, *1*(1), 1–14.

[30] Fisher, J., & Henzinger, T. (2007). Executable cell biology. *Nature Biotechnology*, *25*(11), 1239–1249.

[31] Cazzaniga, P., Damiani, C., Besozzi, D., Colombo, R., Nobile, M., Gaglio, D., ... Vanoni, M. (2014). Computational strategies for a system-level understanding of metabolism. *Metabolites*, *4*(4), 1034–1087.

[32] Feist, A. M., Herrgård, M. J., Thiele, I., Reed, J. L., & Palsson, B. Ø. (2009). Reconstruction of biochemical networks in microorganisms. *Nature Reviews Microbiology*, *7*(2), 129–143.

[33] Thiele, I., & Palsson, B. Ø. (2010). A protocol for generating a high-quality genome-scale metabolic reconstruction. *Nature Protocols*, *5*(1), 93.

[34] Edwards, J. S., & Palsson, B. Ø. (1999). Systems properties of the *Haemophilus influenzae* Rd metabolic genotype. *Journal of Biological Chemistry*, *274*(25), 17410–17416.

[35] Gu, C., Kim, G. B., Kim, W. J., Kim, H. U., & Lee, S. Y. (2019). Current status and applications of genome-scale metabolic models. *Genome Biology*, *20*(1), 121.

[36] Rocha, I., Förster, J., & Nielsen, J. (2008). Design and application of genome-scale reconstructed metabolic models. In *Microbial Gene Essentiality: Protocols and Bioinformatics* (pp. 409–431). Springer.

[37] UniProt: the Universal Protein knowledgebase. (2017). *Nucleic Acids Research*, *45*(D1), D158–D169.

[38] Kanehisa, M., & Goto, S. (2000). KEGG: Kyoto Encyclopedia of Genes and Genomes. *Nucleic Acids Research*, *28*(1), 27–30.

[39] Database Resources of the National Center for Biotechnology Information. (2018). *Nucleic Acids Research*, *46*(D1), D8–D13.

[40] Hucka, M., Bergmann, F. T., Chaouiya, C., Dräger, A., Hoops, S., Keating, S. M., ... Olivier, B. G. et al. (2019). The systems biology markup language (SBML): language specification for level 3 version 2 core release 2. *Journal of Integrative Bioinformatics*, *16*(2).

[41] Wang, H., Marcišauskas, S., Sánchez, B. J., Domenzain, I., Hermansson, D., Agren, R., ... Kerkhoven, E. J. (2018). RAVEN 2.0: A versatile toolbox for metabolic network reconstruction and a case study on *Streptomyces coelicolor*. *PLOS Computational Biology*, *14*(10), e1006541.

[42] Dias, O., Rocha, M., Ferreira, E. C., & Rocha, I. (2010). *Merlin*: Metabolic Models Reconstruction using Genome-Scale Information. *IFAC Proceedings Volumes*, *43*(6), 120–125.

[43] von Kamp, A., Thiele, S., Hädicke, O., & Klamt, S. (2017). Use of CellNetAnalyzer in biotechnology and metabolic engineering. *Journal of Biotechnology*, *261*, 221–228.

[44] Rocha, I., Maia, P., Evangelista, P., Vilaça, P., Soares, S., Pinto, J. P., ... Rocha, M. (2010). OptFlux: an open-source software platform for in silico metabolic engineering. *BMC Systems Biology*, *4*(1), 1–12.

[45] Liao, Y.-C., Tsai, M.-H., Chen, F.-C., & Hsiung, C. A. (2012). GEMSiRV: a software platform for GEnome-scale metabolic model simulation, reconstruction and visualization. *Bioinformatics*, *28*(13), 1752–1758.

[46] Gianchandani, E. P., Chavali, A. K., & Papin, J. A. (2010). The application of flux balance analysis in systems biology. *Wiley Interdisciplinary Reviews: Systems Biology and Medicine*, *2*(3), 372–382.

[47] Raman, K., & Chandra, N. (2009). Flux balance analysis of biological systems: Applications and challenges. *Briefings in Bioinformatics*, *10*(4), 435–449.

[48] Mahadevan, R., & Henson, M. A. (2012). Genome-based modeling and design of metabolic interactions in microbial communities. *Computational and Structural Biotechnology Journal*, *3*(4), e201210008.

[49] Höffner, K., Harwood, S. M., & Barton, P. I. (2013). A reliable simulator for dynamic flux balance analysis. *Biotechnology and Bioengineering*, *110*(3), 792–802.

[50] Balsa-Canto, E., Henriques, D., Gábor, A., & Banga, J. R. (2016b). AMIGO2 Theoretical Background. Retrieved January 29, 2020, from https://sites.google.com/site/amigo2toolbox/doc#AMIGO2_theory.pdf

[51] Balsa-Canto, E., Henriques, D., Gábor, A., & Banga, J. R. (2016c). AMIGO2: Start up guide. Retrieved January 29, 2020, from https://sites.google.com/site/amigo2toolbox/doc#AMIGO2_startup_guide.pdf

[52] MATLAB. (2018). *9.7.0.1190202 (r2019b)*. Natick, Massachusetts: The MathWorks Inc.

[53] Salvadó, Z., Arroyo-López, F., Barrio, E., Querol, A., & Guillamón, J. (2011). Quantifying the individual effects of ethanol and temperature on the fitness advantage of *Saccharomyces cerevisiae*. *Food Microbiology*, *28*(6), 1155–1161.

[54] European Parliament, Council of the European Union. (2003). Retrieved July 13, 2020, from https://eur-lex.europa.eu/legal-content/EN/ALL/?uri=CELEX:32003R1829

[55] Gonzalez, R., Quirós, M., & Morales, P. (2013). Yeast respiration of sugars by non-*Saccharomyces* yeast species: A promising and barely explored approach to lowering alcohol content of wines. *Trends in Food Science & Technology*, *29*(1), 55–61.

[56] Origone, A. C., Rodrıguez, M. E., Oteiza, J. M., Querol, A., & Lopes, C. A. (2018). *Saccharomyces cerevisiae* × *Saccharomyces uvarum* hybrids generated under different conditions share similar winemaking features. *Yeast*, *35*(1), 157–171.

[57] Suárez-Lepe, J., & Morata, A. (2012). New trends in yeast selection for winemaking. *Trends in Food Science & Technology*, *23*(1), 39–50.

[58] Borneman, A. R., Chambers, P. J., & Pretorius, I. S. (2007). Yeast systems biology: modelling the winemaker's art. *Trends in Biotechnology*, *25*(8), 349–355.

[59] Aranda, A., Matallana, E., & Del Olmo, M. (2011). *Saccharomyces* Yeasts I: Primary Fermentation. *Molecular Wine Microbiology*, 1–31.

[60] Pizarro, F., Vargas, F. A., & Agosin, E. (2007). A systems biology perspective of wine fermentations. *Yeast*, *24*(11), 977–991.

[61] Burke, D., Cotter, P., Ross, R., & Hill, C. (2013). Microbial production of bacteriocins for use in foods. In *Microbial production of food ingredients, enzymes and nutraceuticals* (pp. 353–384). Elsevier.

[62] Dobson, P. D., Smallbone, K., Jameson, D., Simeonidis, E., Lanthaler, K., Pir, P., ... Fisher, P. et al. (2010). Further developments towards a genome-scale metabolic model of yeast. *BMC Systems Biology*, *4*(1), 1–7.

[63] Heavner, B. D., Smallbone, K., Barker, B., Mendes, P., & Walker, L. P. (2012). Yeast 5–an expanded reconstruction of the *Saccharomyces cerevisiae* metabolic network. *BMC Systems Biology*, *6*(1), 55.

[64] Heavner, B. D., Smallbone, K., Price, N. D., & Walker, L. P. (2013). Version 6 of the consensus yeast metabolic network refines biochemical coverage and improves model performance. *Database*, *2013*.

[65] Aung, H. W., Henry, S. A., & Walker, L. P. (2013). Revising the representation of fatty acid, glycerolipid, and glycerophospholipid metabolism in the consensus model of yeast metabolism. *Industrial Biotechnology*, *9*(4), 215–228.

[66] Nagelkerke, N. J. et al. (1991). A note on a general definition of the coefficient of determination. *Biometrika*, *78*(3), 691–692.

[67] Solver of nonstiff differential equations - *ode113*. (n.d.). Retrieved July 24, 2020, from https://www.mathworks.com/help/matlab/ref/ode113.html

[68] Shampine, L. F., & Reichelt, M. W. (1997). The MATLAB ODE suite. *SIAM Journal on Scientific Computing*, *18*(1), 1–22.

[69] Lagarias, J. C., Reeds, J. A., Wright, M. H., & Wright, P. E. (1998). Convergence properties of the Nelder–Mead simplex method in low dimensions. *SIAM Journal on Optimization*, *9*(1), 112–147.

[70] Lee, J.-K., Jung, H.-M., & Kim, S.-Y. (2003). 1, 8-dihydroxynaphthalene (DHN)-melanin biosynthesis inhibitors increase erythritol production in *Torula corallina*, and DHN-melanin inhibits erythrose reductase. *Applied and Environmental Microbiology*, *69*(6), 3427–3434.

[71] Liu, X., Yu, X., Wang, Z., Xia, J., Yan, Y., Hu, L., ... Zhao, P. (2020). Enhanced erythritol production by a Snf1-deficient *Yarrowia lipolytica* strain under nitrogen-enriched fermentation condition. *Food and Bioproducts Processing*, *119*, 306–316.

[72] Moon, H.-J., Jeya, M., Kim, I.-W., & Lee, J.-K. (2010). Biotechnological production of erythritol and its applications. *Applied Microbiology and Biotechnology*, *86*(4), 1017–1025.

[73] Park, Y.-C., Lee, D.-Y., Lee, D.-H., Kim, H.-J., Ryu, Y.-W., & Seo, J.-H. (2005). Proteomics and physiology of erythritol-producing strains. *Journal of Chromatography B*, *815*(1-2), 251–260.

[74] Monedero, V., Pérez-Martínez, G., & Yebra, M. J. (2010). Perspectives of engineering lactic acid bacteria for biotechnological polyol production. *Appl Microbiol Biotechnol*, *86*(4), 1003–1015.

[75] Chew, S. Y., Chee, W. J. Y., & Than, L. T. L. (2019). The glyoxylate cycle and alternative carbon metabolism as metabolic adaptation strategies of *Candida glabrata*: Perspectives from *Candida albicans* and *Saccharomyces cerevisiae*. *Journal of Biomedical Science*, *26*(1), 52.

[76] López-Malo, M., Querol, A., & Guillamon, J. M. (2013). Metabolomic comparison of *Saccharomyces cerevisiae* and the cryotolerant species *S. bayanus var. uvarum* and *S. kudriavzevii* during wine fermentation at low temperature. *PLOS ONE*, *8*(3), e60135.

[77] Minebois, R., Pérez-Torrado, R., & Querol, A. (2020a). A time course metabolism comparison among *Saccharomyces cerevisiae*, *S. uvarum* and *S. kudriavzevii* species in wine fermentation. *Food Microbiology*, 103484.

[78] Minebois, R., Pérez-Torrado, R., & Querol, A. (2020b). Metabolome segregation of four strains of *Saccharomyces cerevisiae*, *Saccharomyces uvarum* and *Saccharomyces kudriavzevii* conducted under low temperature oenological conditions. *Environmental Microbiology*, *22*(9), 3700–3721.

[79] Beltran, G., Novo, M., Rozes, N., Mas, A., & Guillamón, J. M. (2004). Nitrogen catabolite repression in *Saccharomyces cerevisiae* during wine fermentations. *FEMS Yeast Research*, *4*(6), 625–632.

[80] Mina, M., & Tsaltas, D. (2017). Contribution of yeast in wine aroma and flavour. *Yeast-Industrial Applications*, 117–134.

[81] Shopska, V., Denkova, R., Lyubenova, V., & Kostov, G. (2019). Kinetic Characteristics of Alcohol Fermentation in Brewing: State of Art and Control of the Fermentation Process. In *Fermented beverages* (pp. 529–575). Elsevier.

[82] Swiegers, J., Bartowsky, E., Henschke, P., & Pretorius, I. (2005). Yeast and bacterial modulation of wine aroma and flavour. *Australian Journal of Grape and Wine Research*, *11*(2), 139–173.

[83] Sudarsan, S., Dethlefsen, S., Blank, L. M., Siemann-Herzberg, M., & Schmid, A. (2014). The functional structure of central carbon metabolism in *Pseudomonas putida* kt2440. *Applied and Environmental Microbiology*, *80*(17), 5292–5303.

[84] Galdieri, L., Zhang, T., Rogerson, D., Lleshi, R., & Vancura, A. (2014). Protein acetylation and acetyl coenzyme a metabolism in budding yeast. *Eukaryotic Cell*, *13*(12), 1472–1483.

[85] Chen, Y., Siewers, V., & Nielsen, J. (2012). Profiling of cytosolic and peroxisomal acetyl-CoA metabolism in *Saccharomyces cerevisiae*. *PLOS ONE*, *7*(8), e42475.

[86] Tronchoni, J., Rozès, N., Querol, A., & Guillamón, J. M. (2012). Lipid composition of wine strains of *Saccharomyces kudriavzevii* and *Saccharomyces cerevisiae* grown at low temperature. *International Journal of Food Microbiology*, *155*(3), 191–198.

[87] Boles, E., de Jong-Gubbels, P., & Pronk, J. T. (1998). Identification and Characterization of MAE1, the *Saccharomyces cerevisiae* Structural Gene Encoding Mitochondrial Malic Enzyme. *Journal of Bacteriology*, *180*(11), 2875–2882.

[88] Ansell, R., Granath, K., Hohmann, S., Thevelein, J. M., & Adler, L. (1997). The two isoenzymes for yeast NAD+-dependent glycerol 3-phosphate dehydrogenase encoded by GPD1 and GPD2 have distinct roles in osmoadaptation and redox regulation. *The EMBO Journal*, *16*(9), 2179–2187.

[89] Bakker, B. M., Overkamp, K. M., van Maris, A. J., Kötter, P., Luttik, M. A., van Dijken, J. P., & Pronk, J. T. (2001). Stoichiometry and compartmentation of NADH metabolism in *Saccharomyces cerevisiae*. *FEMS Microbiology Reviews*, *25*(1), 15–37.

[90] Castegna, A., Scarcia, P., Agrimi, G., Palmieri, L., Rottensteiner, H., Spera, I., ... Palmieri, F. (2010). Identification and functional characterization of a novel mitochondrial carrier for citrate and oxoglutarate in saccharomyces cerevisiae. *Journal of Biological Chemistry*, *285*(23), 17359–17370.

[91] Stincone, A., Prigione, A., Cramer, T., Wamelink, M. M., Campbell, K., Cheung, E., ... Tauqeer Alam, M. et al. (2015). The return of metabolism: Biochemistry and physiology of the pentose phosphate pathway. *Biological Reviews*, *90*(3), 927–963.

[92] Gamero, A., Tronchoni, J., Querol, A., & Belloch, C. (2013). Production of aroma compounds by cryotolerant *Saccharomyces* species and hybrids at low and

moderate fermentation temperatures. *Journal of Applied Microbiology*, *114*(5), 1405–1414.

[93] Kim, S. H., Schneider, B. L., & Reitzer, L. (2010). Genetics and regulation of the major enzymes of alanine synthesis in *Escherichia coli*. *Journal of Bacteriology*, *192*(20), 5304–5311.

[94] Hazelwood, L. A., Daran, J.-M., Van Maris, A. J., Pronk, J. T., & Dickinson, J. R. (2008). The Ehrlich pathway for fusel alcohol production: a century of research on *Saccharomyces cerevisiae* metabolism. *Applied and Environmental Microbiology*, *74*(8), 2259–2266.

[95] Stevens, R. (1961). Formation of phenethyl alcohol and tyrosol during fermentation of a synthetic medium lacking amino-acids. *Nature*, *191*(4791), 913–914.

[96] Crépin, L., Truong, N. M., Bloem, A., Sanchez, I., Dequin, S., & Camarasa, C. (2017). Management of multiple nitrogen sources during wine fermentation by *Saccharomyces cerevisiae*. *Applied and Environmental Microbiology*, *83*(5).

[97] Camarasa, C., Grivet, J.-P., & Dequin, S. (2003). Investigation by 13C-NMR and tricarboxylic acid (TCA) deletion mutant analysis of pathways for succinate formation in *Saccharomyces cerevisiae* during anaerobic fermentation. *Microbiology*, *149*(9), 2669–2678.

[98] Bach, B., Meudec, E., Lepoutre, J.-P., Rossignol, T., Blondin, B., Dequin, S., & Camarasa, C. (2009). New insights into γ-aminobutyric acid catabolism: evidence for γ-hydroxybutyric acid and polyhydroxybutyrate synthesis in *Saccharomyces cerevisiae*. *Applied and Environmental Microbiology*, *75*(13), 4231–4239.

[99] Cao, J., Barbosa, J. M., Singh, N. K., & Locy, R. D. (2013). GABA shunt mediates thermotolerance in *Saccharomyces cerevisiae* by reducing reactive oxygen production. *Yeast*, *30*(4), 129–144.

[100] Tippmann, S., Chen, Y., Siewers, V., & Nielsen, J. (2013). From flavors and pharmaceuticals to advanced biofuels: Production of isoprenoids in *Saccharomyces cerevisiae*. *Biotechnology Journal*, *8*(12), 1435–1444.

[101] Bröker, J. N., Müller, B., van Deenen, N., Prüfer, D., & Gronover, C. S. (2018). Upregulating the mevalonate pathway and repressing sterol synthesis in *Saccharomyces cerevisiae* enhances the production of triterpenes. *Applied Microbiology and Biotechnology*, *102*(16), 6923–6934.

[102] Klug, L., & Daum, G. (2014). Yeast lipid metabolism at a glance. *FEMS Yeast Research*, *14*(3), 369–388.

[103] Kuranda, K., François, J., & Palamarczyk, G. (2009). The isoprenoid pathway and transcriptional response to its inhibitors in the yeast *Saccharomyces cerevisiae*. *FEMS Yeast Research*, *10*(1), 14–27.

[104] Coleman, S. T., Fang, T. K., Rovinsky, S. A., Turano, F. J., & Moye-Rowley, W. S. (2001). Expression of a glutamate decarboxylase homologue is required for normal oxidative stress tolerance in *Saccharomyces cerevisiae*. *Journal of Biological Chemistry*, *276*(1), 244–250.

[105] Bruinenberg, P. M., de Bot, P. H., van Dijken, J. P., & Scheffers, W. A. (1983). The role of redox balances in the anaerobic fermentation of xylose by yeasts. *European Journal of Applied Microbiology and Biotechnology*, *18*(5), 287–292.

[106] Van Dijken, J. P., & Scheffers, W. A. (1986). Redox balances in the metabolism of sugars by yeasts. *FEMS Microbiology Reviews*, *1*(3-4), 199–224.

[107] Herrero, E., Ros, J., Bellı, G., & Cabiscol, E. (2008). Redox control and oxidative stress in yeast cells. *Biochimica et Biophysica Acta (BBA)-General Subjects*, *1780*(11), 1217–1235.

[108] Beltran, G., Novo, M., Leberre, V., Sokol, S., Labourdette, D., Guillamon, J.-M., ... Rozes, N. (2006). Integration of transcriptomic and metabolic analyses for understanding the global responses of low-temperature winemaking fermentations. *FEMS Yeast Research*, *6*(8), 1167–1183.

[109] Bertolini, L., Zambonelli, C., Giudici, P., & Castellari, L. (1996). Higher alcohol production by cryotolerant *Saccharomyces* strains. *American Journal of Enology and Viticulture*, *47*(3), 343–345.

[110] Noble, A., & Bursick, G. (1984). The contribution of glycerol to perceived viscosity and sweetness in white wine. *American Journal of Enology and Viticulture*, *35*(2), 110–112.

[111] Fernandes, N. C. M., Gomes, F. d. C. O., Garcia, C. F., Vieira, M. d. L. A., & Machado, A. M. d. R. (2018). Use of solid phase microextraction to identify volatile organic compounds in brazilian wines from different grape varieties. *Brazilian Journal of Food Technology*, *21*.

[112] Tronchoni, J., Medina, V., Guillamón, J. M., Querol, A., & Pérez-Torrado, R. (2014). Transcriptomics of cryophilic *Saccharomyces kudriavzevii* reveals the key role of gene translation efficiency in cold stress adaptations. *BMC Genomics*, *15*(1), 432.

NB: This work was supported by a grant of CSIC (Consejo Superior de Investigaciones Científicas), the “JAE Intro ICUs 2019” grant: JAEICU-19-IIM-01, in Instituto de Investigaciones Marinas - CSIC (IIM-CSIC).